AFGL-TR-78-0154

LEVEL II

INFRARED ABSORPTION BY CO_2 and H_2O

David A. Gryvnak
Darrell E. Burch

Ford Aerospace and Communications Corporation
Aeronutronic Division
Ford Road, Newport Beach, CA 92663

May 1978

Scientific Report for Period 4 October 1976 - 4 October 1977

Approved for public release; distribution unlimited

AIR FORCE CAMBRIDGE RESEARCH LABORATORIES
AIR FORCE SYSTEMS COMMAND
UNITED STATES AIR FORCE
HANSCOM AFB, MASSACHUSETTS 01731

SECURITY CLASSIFICATION OF THIS PAGE (When Data Entered)

REPORT DOCUMENTATION PAGE

READ INSTRUCTIONS BEFORE COMPLETING FORM

1. REPORT NUMBER	2. GOVT ACCESSION NO.	3. RECIPIENT'S CATALOG NUMBER
AFGL-TR-78-0154		

4. TITLE (and Subtitle)

INFRARED ABSORPTION BY CO_2 and H_2O

5. TYPE OF REPORT & PERIOD COVERED

Scientific Report No. 1

~~10/04/76-10/04/77~~

6. PERFORMING ORG. REPORT NUMBER

U-6417

7. AUTHOR(s)

David A. Gryvnak
Darrell E. Burch

8. CONTRACT OR GRANT NUMBER(s)

F19628-76-C-0302

9. PERFORMING ORGANIZATION NAME AND ADDRESS

Ford Aerospace and Communications Corporation
Aeronutronic Division
Ford Road, Newport Beach, CA 92663

10. PROGRAM ELEMENT, PROJECT, TASK AREA & WORK UNIT NUMBERS

62101F
767009AJ

11. CONTROLLING OFFICE NAME AND ADDRESS

Air Force Geophysics Laboratories
Hanscom AFB, Massachusetts 01731
Contract Monitor: Anthony P. D'Agati

12. REPORT DATE

May 1978

13. NUMBER OF PAGES

59

14. MONITORING AGENCY NAME & ADDRESS (if different from Controlling Office)

15. SECURITY CLASS. (of this report)

Unclassified

15a. DECLASSIFICATION/DOWNGRADING SCHEDULE

16. DISTRIBUTION STATEMENT (of this Report)

Approved for public release; distribution unlimited.

17. DISTRIBUTION STATEMENT (of the abstract entered in Block 20, if different from Report)

18. SUPPLEMENTARY NOTES

19. KEY WORDS (Continue on reverse side if necessary and identify by block number)

H_2O, CO_2
Atmospheric Transmission
Absorption
Continuum Absorption
Line Shape

20. ABSTRACT (Continue on reverse side if necessary and identify by block number)

Spectral transmission data for CO_2 are presented between approximately 495 and 835 cm^{-1} for a variety of samples of CO_2 mixed in dry air. Sample parameters cover a wide range of pressures with the temperatures near 310 K. The spectral resolution varies from approximately 0.4 to 0.6 cm^{-1}. Also included are data on the continuum absorption by H_2O between 300 and 825 cm^{-1}. Experimental data on H_2O absorption are compared with data calculated on the basis of several theoretical line shapes. The H_2O continuum absorption decreases more rapidly with increasing temperature than is predicted by line-shape theories.

DD FORM 1 JAN 73 1473 EDITION OF 1 NOV 68 IS OBSOLETE

SECURITY CLASSIFICATION OF THIS PAGE (When Data Entered)

TABLE OF CONTENTS

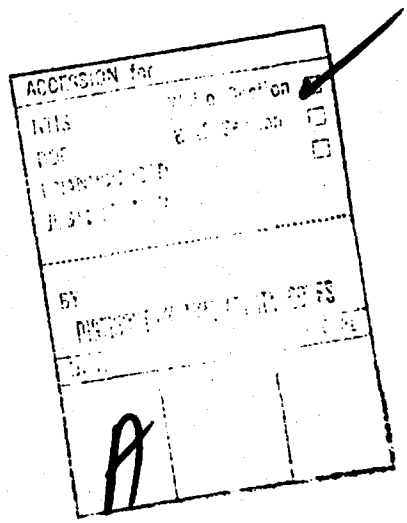

SECTION 1

INTRODUCTION

The experimental work reported herein has been performed primarily to obtain detailed absorption data to use as a check for the AFGL line-parameter listing[1] and to serve as a basis for possible modifications to the listing. Section 2 provides extensive data that can be used to check the intensities, widths and shapes of the CO_2 lines in the important 15 um band. Accurate information on these parameters is required because of the use of this band in remote sensing of the atmosphere from satellite-borne instruments and ground based instruments. The CO_2 data included in this report complement the data presented by us in a previous report.[2]

Section 3 shows several comparisons of calculated spectra with experimental spectra on the absorption by H_2O between approximately 330 cm^{-1} and 600 cm^{-1}. Most of the experimental data used in the comparison were obtained by us and reported previously.[2-4] Theoretical intensities, widths and positions of most of the H_2O absorption lines agree quite well with the experimental results. The most serious discrepancies occur in the intervals that are several cm^{-1} from the nearest line of significant strength. The discrepancy is worse for samples of pure H_2O than for samples of $H_2O + N_2$. This portion of the study is not yet complete. Additional work will be presented in a later report.

---

1. R. A. McClatchey, W. S. Benedict, S. A. Clough, D. E. Burch, R. F. Calfee K. Fox, L. S. Rothman, and J. S. Garing; "AFCRL Atmospheric Absorption Line Parameters Compilation", AFCRL-TR-73-0096, 26 January 1973. (Associated with this report is a magnetic tape listing the line parameters.)

2. David A. Gryvnak, Darrell E. Burch, Robert L. Alt, and Dorianne K. Zgonc; "Infrared Absorption by CH_4, H_2O and CO_2", Final Report No. AFGL-TR-76-0246 on Contract F19628-76-C-0067. Aeronutronic Report No. U-6275, December 1977.

3. Darrell E. Burch, David A. Gryvnak, and Francis J. Gates; "Continuum Absorption by H_2O Between 330 and 825 cm^{-1}", Final Report No. AFCRL-TR-74-0377 on Contract F19628-74-C-0069. Aeronutronic Report No. U-6095, September 1974.

4. Darrell E. Burch, David A. Gryvnak, and John D. Pembrook; "Infrared Absorption by H_2O, NO_2, and N_2O_4", Final Report No. AFCRL-TR-75-0420 on Contract No. F19628-75-C-0049. Aeronutronic Report No. U-6159, September 1975.

DEFINITIONS, SYMBOLS, AND NOMENCLATURE

The true transmittance of a gas sample that would be observed at wavenumber ν with infinite resolving power is given by

$$T' = \exp(-u\alpha), \quad \text{or} \quad (-1/u)\ln T' = \alpha. \tag{1}$$

The absorption coefficient α has units consistent with u, which is defined by Equation (2). Because of the finite slitwidth of a spectrometer and variations in α with wavenumber due to line structure, the observed transmittance T may differ from T' at the same wavenumber. The quantity T represents a weighted average of T' over the interval passed by the spectrometer.

The absorber thickness, u, of a gas sample is given by

$$u(\text{molecules/cm}^2) = 2.69 \times 10^{19}\ p^*\ (\text{atm})\ L(\text{cm})\ (273/\theta),$$

$$= 7.34 \times 10^{21}\ p^*\ (L/\theta). \tag{2}$$

The temperature θ is in degrees Kelvin, and L is the geometrical path length through the sample. The density-equivalent-pressure p* of the absorbing gas may vary slightly from the partial pressure p at high pressures. The gas does not follow exactly the perfect gas law at the higher pressures for which the Van der Waals' equation of state is required. The deviation from the perfect gas law causes a non-linear relationship between the pressure and the density of the gas. For all of the pressures used in the present investigation, the following simple expression is sufficiently accurate:

$$p^* = p(1 + c\ p). \tag{3}$$

The pressures are in atm, and c depends on the gas species and temperature. Near room temperature, $c \approx 0.005\ \text{atm}^{-1}$ for CO_2. For the H_2O samples studied, the difference between p* and p can be ignored.

Because of differences in the efficiencies of collisions with molecules of different gas species, the half-width α of a collision-broadened line depends on the partial pressure of each of the gas species present in a sample. The equivalent pressure P_e given by the following equation is a convenient parameter when dealing with absorption by a mixture that contains non-absorbing N_2 in addition to the absorbing gas species:

$$P_e = Bp + p_N = (B-1)p + P, \tag{4}$$

where P is the total pressure, p_N is the partial pressure of N_2, and p is the partial pressure of the absorbing gas species. The experimentally determined constant B is the ratio of the self-broadening ability to the broadening

ability of N_2. The equivalent pressure is therefore directly proportional to α, regardless of the relative concentrations of the absorbing gas and the N_2. We note that P_e approximates P for dilute mixtures of the absorbing gas species in N_2 ($p \ll p_N$). The CO_2 samples discussed in Section 2 consisted of CO_2 plus dry air; the dry air consisted of 79% N_2 and 21% O_2 to closely approximate the atmosphere. The same symbol, P_e, represents the equivalent pressure of these samples with p_{air} replacing p_N in Eq. (4).

Because of the proportional relationship between α and pressure, the absorption coefficient k due to a single absorption line is also proportional to pressure in the extreme wings of a line where $|\nu - \nu_o| \gg \alpha$. This linear relationship between pressure of a sample of fixed composition and the absorption coefficient in the wings has been demonstrated experimentally under many conditions; it is also predicted by most theoretical line shapes. It follows that the wing absorption coefficient C due to the extreme wings of several lines is proportional to pressure and is equal to the sum of all of the individual absorption coefficients (denoted by k) due to each line. Because wing absorption changes slowly with wavenumber, it is frequently called continuum absorption. Continuum absorption may also arise from dimers, such as $H_2O{:}H_2O$, or from pressure-induced bands. These two types of continuum have the same pressure dependence as absorption by line wings; therefore, in some cases we cannot distinguish which is the source of the absorption being measured.

The absorption coefficient due to local lines whose centers occur within a few cm^{-1} of the point of observation is denoted by κ(local). This quantity may vary rapidly with wavenumber and depends on pressure because of collision-broadening of the absorption lines. At a given wavenumber, there may be absorption by local lines as well as by continuum. Therefore, for a pure H_2O sample, the total absorption coefficient κ in Eq. (1) is given by

$$\kappa = \kappa(\text{local}) + C_s^o\, p. \qquad (\text{pure } H_2O) \qquad (5)$$

The normalized continuum coefficient C_s^o is the value of C_s at a given temperature when p = 1 atm. The subscript s denotes self-broadening of the lines. Since α_s^o is proportional to p, and u is proportional to pL, it follows that $(-\ell_n T)$ for continuum due to the wings of lines is proportional to p^2L.

For a mixture of $H_2O + N_2$, Eq. (5) must be modified to account for broadening of the H_2O lines by N_2.

$$\kappa = \kappa(\text{local}) + C_s^o\, p + C_N^o\, p_N\,. \qquad (6)$$

Several different line shapes have been proposed for collision-broadened absorption lines. Some of the most widely used shapes are represented by Eqs. (7) - (11). Each of these theoretical shapes has an apparent deficiency under some condition. Nevertheless, it is informative to compare the absorption coefficients predicted by the different shapes in different portions of the

spectrum. Near the line center where $|\nu - \nu_o| \ll \nu_o$ and $|\nu - \nu_o|$ is not more than a few times α, values of k given by all of the equations approach the value given by the simple Lorentz equation.

$$k = \frac{S}{\pi} \frac{\alpha}{(\nu-\nu_o)^2 + \alpha^2} \qquad \text{Simple Lorentz} \qquad (7)$$

$$= \frac{S}{\pi} \frac{\nu}{\nu_o} \left[\frac{\alpha}{(\nu-\nu_o)^2 + \alpha^2} - \frac{\alpha}{(\nu+\nu_o)^2 + \alpha^2} \right] \qquad \text{Full Lorentz} \qquad (8)$$

$$= \frac{S}{\pi} \frac{\nu}{\nu_o}^2 \left[\frac{\alpha}{(\nu-\nu_o)^2 + \alpha^2} + \frac{\alpha}{(\nu+\nu_o)^2 + \alpha^2} \right] \qquad \text{VVW} \qquad (9)$$

$$= \frac{S}{\pi} \frac{\nu}{\nu_o} \frac{1 - \exp(-ch\nu/\mathscr{k}\theta)}{1 - \exp(-ch\nu_o/\mathscr{k}\theta)} \left[\frac{\alpha}{(\nu-\nu_o)^2 + \alpha^2} + \frac{\alpha}{(\nu+\nu_o)^2 + \alpha^2} \right] \qquad \text{MVVW} \qquad (10)$$

$$= \frac{S}{\pi} \frac{4\nu^2\alpha}{(\nu^2-\nu_o^2)^2 + 4\nu^2\alpha^2} \qquad \text{Gross}^5 \qquad (11)$$

The names commonly associated with each of the shapes are indicated. Van Vleck-Weisskopf and modified Van Vleck-Weisskopf are abbreviated by VVW and MVVW, respectively. The line center is indicated by ν_o, the line intensity by S, the speed of light by c, Boltzmann's constant by script $\mathscr{k}$, Planck's constant by h, and temperature (in Kelvins) by θ.

Consider the continuum at a wavenumber where the absorption is due to the wings ($|\nu - \nu_o| \gg \alpha$) of several lines the shapes of which are given by any one of the equations above. It follows from the above discussion that C_s^o/C_N^o would be equal the ratio α_s^o/α_N^o of the normalized half-widths for self-broadening and N_2 broadening. Previous results of measurements at wavenumbers where most of the absorption is due to H_2O lines centered between approximately 1 and 20 cm^{-1} away from the point of the measurement indicate that this ratio is approximately 5. However, at wavenumbers where much of the absorption is apparently due to more distant lines, the ratio C_s^o/C_N^o may be much greater than 5. These results indicate that the shapes of the extreme wings of self-broadened H_2O lines are different from those of N_2-broadened H_2O lines. This subject is treated in considerable detail in Section 3.

---

5. E. P. Gross, Phys. Rev. 97, 395 (1955).

SECTION 2

ABSORPTION BY CO_2 BETWEEN 500 AND 850 cm^{-1}

BACKGROUND

In a previous report[2], we presented spectral data on the absorption by CO_2 between 500 and 850 cm^{-1} for samples covering wide ranges of temperature, pressure and absorber thickness. The major purpose for these data was to provide a means of checking the intensitites, widths, and shapes of the CO_2 absorption lines in this spectral region. The line parameters are checked by comparing the spectral curves of transmittance obtained experimentally with calculated curves for an identical sample based on the line parameters on the AFGL line parameters tape. At any wavenumber the absorption may be due to several different lines from different bands. In many cases, the relative contributions by the various bands depend on the sample parameters temperature, pressure and absorber thickness. Thus, by varying each of these sample parameters over a wide range of values, the line parameters can be checked by comparing the experimental data with the calculated spectra.

The experimental data presented in the previous report were obtained with spectral slitwidths between approximately 1.2 cm^{-1} and 4.2 cm^{-1}. The resolution was coarse enough to smooth-out most of the structure due to the individual lines in the P- and R-branches of the strong bands. The strong Q-branches were still quite apparent in many of the spectra, but the contours of the curves over the Q-branches were distorted significantly by the relatively coarse resolution. A few of the calculated spectra differed significantly from the corresponding experimental data, particularly near some of the Q-branches. Upon comparing the data, it became apparent that many of the line parameters could be checked more accurately with experimental spectra of several selected samples that were obtained with higher resolution. The data presented in this section were obtained for this purpose.

The spectral regions chosen for the additional study with higher resolution contain features, such as a weak Q-branch, that could not be observed accurately with coarse resolution. The sample parameters were selected so these features could be observed best. For example, a very weak Q-branch may not be observable in a coarse-resolution spectrum because it occurs among the P- or R-branch lines of a stronger band. However, the weak Q-branch can be made to stand out in a higher-resolution spectrum of a sample at low pressure. The amount of absorption by the many very weak lines in a Q-branch is much higher relative to that by stronger, well-separated lines for a low-pressure sample than for a high-pressure sample. Spectra were also obtained for a few high-pressure samples to provide information on the intensities of a few spectral features and on the shapes of the extreme wings of the absorption lines.

EXPERIMENTAL

The experimental procedures were similar to those employed previously. All samples consisted of either pure CO_2 or of CO_2 plus dry air; the dry air consisted of 79% N_2 and 21% O_2 to match the atmosphere. The mixtures of CO_2 plus dry air were obtained pre-mixed from a commercial gas supplier in cylinders at total pressures of approximately 150 atm. Table 1 lists the mole concentrations of the CO_2 in the different mixtures studied. A concentration of 1.000 corresponds to pure CO_2; 0.153 corresponds to 15.3% CO_2 plus 84.7% dry air, etc. The concentration of each mixture was determined in the previous study.[2]

All of the samples were contained in a multiple-pass absorption cell with a base length of approximately 1 meter. The pathlength L through each sample is given in Table 1. Sample temperatures were maintained between 308 and 311 K to correspond approximately to the highest temperatures encountered in the atmosphere. The temperature of a given sample was uniform to less than $\pm$ 1 K throughout the length of the cell. Also given in Table 1 are: the absorber thickness u, the CO_2 partial pressure p, and the equivalent pressure P_e ($= P + 0.30\ p$). The number of the figure in which the spectrum appears is given in the right-hand column of Table 1. The spectral region over which each sample was studied is also given in Table 1 along with the Resolution Schedule.

Table 2 relates the Resolution Schedule to the spectral slitwidth, which is based on a "triangular slit-function" and is equal to the full width of the triangle at half maximum. A grating with 40 grooves/mm was employed to obtain Resolution Schedules A and B; the grating used for Resolution Schedule C contained 75 grooves/mm.

The procedures employed in scanning and analyzing the spectral data are essentially the same as those used previously.[2] All of the optical path external to the sample cell passed either through a vacuum or through non-absorbing N_2 to eliminate absorption by CO_2 or any other atmospheric gas. A Nernst glower served as the source of radiant energy. The detector contained a sensitive element of Ge:Cu and was cooled by liquid He.

A background curve that corresponded to 100% transmittance was scanned with the sample cell evacuated, either immediately before or after each sample spectrum was scanned. In order to check for possible sampling errors or changes in the signal level corresponding to 100% transmittance during a scan, portions of each spectrum were re-run and the results were compared with the spectrum that was to be reduced further. Separate samples having the same parameters were employed in the comparisons as further checks for possible sampling errors. Each sample spectrum and its corresponding background spectrum were digitized with the data related directly to detector signal punched on computer cards. A computer then calculated values of transmittance, integrated absorptance, etc.

Tables 3 and 4 list the absorption lines used to provide wavenumber

TABLE 1. SAMPLE PARAMETERS

Sample No.	CO_2 Conc.	T (K)	L (cm)	p (atm)	P (atm)	P_e (atm)	$\left(\frac{u}{\frac{molecules}{cm^2}}\right)$	Spectral Range (cm^{-1})	Res. Sch.	Fig. No.
HR01	1.000	308	3291	7.697E 00	7.697E 00	1.037E 01	6.258E 23	494- 512	A	1
HR02	1.000	308	3291	3.000E 00	3.000E 00	3.955E 00	2.387E 23	494- 512	A	1
HR03	0.153	308	3291	1.460E 00	9.539E 00	9.990E 00	1.153E 23	494- 512	A	1
HR04	0.153	308	3291	4.590E-01	3.000E 00	3.139E 00	3.609E 22	494- 512	A	1
HR05	1.000	310	3291	7.697E-01	7.697E-01	1.004E 00	6.023E 22	494- 580	A	1,2,3
HR06	1.000	310	3291	1.921E-01	1.921E-01	2.500E-01	1.499E 22	542- 550	A	3
HR07	0.153	310	3291	1.462E-01	9.553E-01	9.992E-01	1.140E 22	542- 550	A	3
HR08	0.153	310	3291	3.644E-02	2.382E-01	2.491E-01	2.841E 21	542- 550	A	3
HR09	1.000	310	3291	3.000E 00	3.000E 00	3.955E 00	2.372E 23	535- 552	A	4
HR10	1.000	308	416	7.697E 00	7.697E 00	1.037E 01	7.911E 22	535- 552	A	4
HR11	0.153	309	3291	1.460E 00	9.539E 00	9.990E 00	1.149E 23	535- 552	A	4
HR12	0.153	309	826	1.460E 00	9.539E 00	9.990E 00	2.894E 22	535- 552	A	4
HR13	0.153	308	3291	4.389E-01	2.868E 00	3.001E 00	3.451E 22	535- 552	A	4
HR14	1.000	308	3291	2.408E-02	2.408E-02	3.131E-02	1.890E 21	567- 632	B	5
HR15	0.153	310	3291	1.464E-01	9.566E-01	1.001E 00	1.142E 22	567- 632	B	5
HR16	0.153	310	3291	3.664E-02	2.395E-01	2.505E-01	2.857E 21	567- 632	B	5
HR17	0.00500	310	1648	5.000E-03	1.000E 00	1.002E 00	1.952E 20	567- 632	B	5
HR18	0.00125	310	1648	1.250E-02	1.000E 01	1.000E 01	4.880E 20	611- 632	B	6
HR19	0.00125	310	1648	3.750E-03	3.000E 00	3.001E 00	1.464E 20	611- 632	B	6
HR20	0.00125	310	1648	1.250E-03	1.000E 00	1.000E 00	4.880E 19	611- 632	B	6
HR21	0.153	308	3291	4.570E-03	2.987E-02	3.124E-02	3.586E 20	611- 632	B	6
HR22	1.000	310	1648	6.053E-03	6.053E-03	7.869E-03	2.369E 20	611- 632	B	6
HR23	0.153	310	3291	4.570E-03	2.987E-02	3.124E-02	3.563E 20	610- 775	C	7,8
HR24	1.000	310	3291	1.092E-03	1.092E-03	1.420E-03	8.514E 19	640- 680	C	9
HR25	0.153	310	3291	2.939E-04	1.921E-03	2.009E-03	2.291E 19	640- 680	C	9
HR26	0.00125	311	826	1.250E-03	1.000E 00	1.000E 00	2.438E 19	640- 680	C	9
HR27	0.000312	311	826	3.120E-04	1.000E 00	1.000E 00	6.085E 18	640- 680	C	9
HR28	0.000039	311	826	3.910E-05	1.000E 00	1.000E 00	7.626E 17	640- 680	C	9
HR29	0.153	314	826	1.530E-01	1.000E 00	1.046E 00	2.958E 21	705- 770	C	10
HR30	0.00977	314	826	9.731E-03	9.961E-01	9.990E-01	1.880E 20	705- 770	C	10
HR31	0.00125	311	1648	1.250E-02	1.000E 01	1.000E 01	4.865E 20	705- 770	C	10
HR32	0.00125	311	1648	3.750E-03	3.000E 00	3.001E 00	1.459E 20	705- 770	C	10
HR33	0.00125	311	1648	1.250E-03	1.000E 00	1.000E 00	4.864E 19	705- 770	C	10
HR34	1.000	311	1648	4.803E-02	4.803E-02	6.245E-02	1.869E 21	705- 775	C	11
HR35	1.000	311	1648	6.079E-03	6.079E-03	7.903E-03	2.366E 20	705- 775	C	11
HR36	0.153	310	3291	1.147E-03	7.500E-03	7.844E-03	8.946E 19	705- 775	C	11
HR37	1.000	311	3291	7.347E 00	7.347E 00	9.881E 00	5.907E 23	775- 838	C	12
HR38	1.000	311	3291	2.279E 00	2.279E 00	2.994E 00	1.790E 23	775- 838	C	12
HR39	1.000	310	3291	7.697E-01	7.697E-01	1.004E 00	6.023E 22	775- 838	C	12
HR40	0.0385	311	3291	3.850E-01	1.000E 01	1.012E 01	2.997E 22	775- 838	C	12
HR41	0.00977	311	3291	9.770E-02	1.000E 01	1.003E 01	7.596E 21	775- 838	C	12
HR42	1.000	311	3291	1.921E-01	1.921E-01	2.500E-01	1.494E 22	775- 838	C	13
HR43	0.153	311	3291	1.464E-01	9.566E-01	1.001E 00	1.138E 22	775- 838	C	13
HR44	1.000	311	3291	4.803E-02	4.803E-02	6.245E-02	3.733E 21	775- 838	C	13
HR45	0.0385	311	3291	3.804E-02	9.882E-01	9.996E-01	2.957E 21	775- 838	C	13

TABLE 2. RESOLUTION SCHEDULES

ν (cm^{-1})	Spectral resolution A (cm^{-1})	B (cm^{-1})	C (cm^{-1})
500	0.41		
520	0.44		
540	0.48		
560	0.52	0.42	
580		0.45	
600		0.49	0.26
620		0.53	0.28
640		0.57	0.31
660		0.61	0.33
680			0.36
700			0.38
720			0.41
740			0.43
760			0.46
780			0.49
800			0.51
820			0.54
840			0.57

TABLE 3. CALIBRATION DATA FOR 494-632 cm^{-1} REGION

ν_o (cm^{-1})	Gas (b)	Reference (a)	ν_o (cm^{-1})	Gas (b)	Reference (a)
486.14	H_2O	BC	555.85	Int	
488.13	Int		557.07	Int	
490.13	Int		558.29	Int	
492.15	Int		559.53	Int	
494.19	H_2O	BC	560.76	Int	
496.18	Int		562.00		
498.19	Int		563.25	H_2O	BC
500.22	Int		567.23	H_2O	BC
502.26	H_2O	AF	569.27	H_2O	BC
504.45	H_2O	AF	571.35	H_2O	AF
506.93	H_2O	BC	576.11	H_2O	AF
509.36	Int		578.26	Int	
511.82	Int		580.41	Int	
514.30	Int		582.56	Int	
516.82	H_2O	BC	584.71	H_2O	AF
519.60	H_2O	BC	587.26	Int	
521.70	Int		589.81	Int	
523.84	Int		592.37	Int	
525.98	H_2O	BC	594.96	H_2O	BC
528.00	Int		600.11	H_2O	BC
530.04	Int		604.45	H_2O	BC
532.09	Int		606.76	Int	
534.17	Int		609.07	Int	
536.26	H_2O	BC	611.39	Int	
541.07	H_2O	AF	613.75	Int	
545.30	H_2O	BC	616.07	H_2O	BC
546.30	H_2O	BC	620.57	H_2O	BC
547.83	H_2O	BC	625.29	H_2O	BC
549.98	H_2O	BC	628.12	Int	
554.64	H_2O	BC	630.98	Int	
			633.87	CO_2	D

(a) BC indicates that the center positions of the H_2O lines are from unpublished data by Benedict and Calfee (Ref. 6). D indicates that the center position of the CO_2 line is from Drayson (Ref. 7). AF refers to the AFGL line-parameters listing.

(b) Int denotes the positions of calibration points found by interpolation as discussed in the text.

calibration. Transmission spectra of appropriate samples of the calibration gas, either CO_2 or H_2O, were scanned with spectral slitwidths equal to or narrower than those used to obtain the data. Positions of the centers of the calibration lines were determined in terms of fiducial marks that were related directly to grating position. Absorption lines of H_2O were employed for the low-wavenumber side of the region from 486 cm^{-1} to 625 cm^{-1}. The H_2O lines used are reasonably well isolated from other lines so that the center positions could be located accurately, and the points of maximum abosrption were nearly independent of the slitwidth. Many of the CO_2 lines in the 490-625 cm^{-1} region are blended, making it difficult to determine their center positions accurately. All of the H_2O line positions from 486.14 to 625.29 cm^{-1} are from unpublished data provided by Benedict and Calfee.[6] The values listed for these lines agree within a few hundredths of a cm^{-1} with the corresponding values in the AFGL listing of line parameters.[1]

The CO_2 line positions are well-known[7] throughout most of the spectral region and were used from approximately 609 cm^{-1} to the high-wavenumber side of the band system. Three H_2O lines centered between 616 cm^{-1} and 626 cm^{-1} were used because their positions could be determined more accurately than those of nearby CO_2 lines. Most of the CO_2 lines listed in Table 4 are not "blended" enough with weaker adjacent lines to shift the apparent line centers significantly.

The computer program used to reduce the data has been written so that wavenumbers between the calibration lines are calculated on the basis of a linear relationship between wavenumber and the fiducial marks that indicate the grating position. On the original spectra as they are scanned by the spectrometer, the wavenumber scale deviates enough from this linear relationship to cause a significant error in the final calculated spectrum if the calibration lines are too far apart. In order to reduce such errors, we have generated additional calibration points between the CO_2 or H_2O calibration lines listed in Tables 3 and 4. These generated calibration points, indicated by "Int" in the tables, were determined by employing a second-order equation to interpolate between the CO_2 or H_2O calibration lines. If this more accurate method of interpolation had not been employed, systematic calibration errors as large as approximately 0.1 cm^{-1} would have resulted in some places. With the accurately interpolated calibration points, any systematic errors resulting

---

6. W. S. Benedict, Inst. for Molecular Physics, College Park Maryland, 90742; R. Calfee, Wave Propogation Labs., Environmental Research Labs, National Oceanic Atmospheric Administration, Boulder Colorado 80302 (Private Communication).

7. S. R. Drayson, "A Listing of Wavenumbers and Intensities of Carbon Dioxide Absorption Lines Between 12 and 20 μm". Technical Report 036350-4-T, National Aeronautics and Space Administration, Contract No. NSR 23-005-376, May 1973.

TABLE 4. CALIBRATION DATA FOR 610-838 cm^{-1} REGION

ν_o (cm^{-1})	Gas (b)	Band (c)	Line	Ref. (a)
609.42	CO_2	2	P11	D
616.07	H_2O			BC
620.57	H_2O			BC
625.27	H_2O			BC
629.44	CO_2	1	P50	D
636.85	CO_2	1	P40	D
639.81	Int			
642.80	Int			
645.86	CO_2	1	P28	D
648.87	Int			
651.92	Int			
655.00	CO_2	1	P16	D
661.16	CO_2	1	P8	D
665.51	Int			
669.93	Int			
674.44	C_2O_2	1	R8	D
679.19	CO_2	1	R14	D
687.16	CO_2	1	R24	D
690.33	Int			
693.54	Int			
696.78	Int			
700.06	CO_2	1	R40	D
706.58	CO_2	1	R48	D
713.13	CO_2	1	R56	D
716.17	Int			
719.25	Int			D
722.35	Int			
725.47	CO_2	3	R5	
734.71	CO_2	3	R17	D
743.83	CO_2	3	R29	
751.34	CO_2	3	R39	D
755.81	CO_2	3	R45	D
760.27	CO_2	3	R51	D
766.28	CO_2		W (d)	
777.37	CO_2	6	P18	
788.32	CO_2	6	P4	D
798.47	CO_2	6	R8	D
806.26	CO_2	6	R18	D
812.48	CO_2	6	R26	D
820.27	CO_2	6	R36	D
826.51	CO_2	6	R44	D
831.22	CO_2	6	R50	D
836.05	CO_2		W (d)	
842.04	Ext			

(a) D and BC indicate that the positions of the line centers are from Drayson (Ref. 7) or Benedict and Calfee (Ref. 6), respectively.

(b) CO_2 and H_2O refer to the gas used for calibration. Int or Ext denotes the positions of calibration points found by interpolation or extrapolation, respectively, as discussed in the text.

(c) The CO_2 bands are identified by the energy levels involved and the band centers in the following table. All bands correspond to the most common isotope, $^{16}O\ ^{12}C\ ^{16}O$.

Band No.	Energy Levels			ν_c (cm^{-1})
1	010:0	←	000:0	667.381
2	(100:0) II	←	010:1	618.029
3	(100:0) I	←	010:1	720.805
6	(110:1) I	←	(100:0)II	791.446
8	(110:1) I	←	020:2	741.724
13	(120:2) I	←	(110:1)II	828.230

(d) The W corresponding to the calibration point at 766.28 cm^{-1} represents a weighted average of the positions of four CO_2 lines centered at 766.151, 766.190, 766.430, and 766.438 cm^{-1}. Similarly the point at 836.05 cm^{-1} represents a weighted average of two lines centered at 835.951 and 836.132 cm^{-1}. Each line has been weighted in proportion to its intensity.

from the linear-wavenumber interpolation performed by the computer are no greater than approximately 0.002 to 0.03 cm^{-1}. Such errors are smaller than other errors involved in the calibration. In some of the intervals between adjacent CO_2 or H_2O lines, more interpolated calibrations points were used than were required to produce the desired accuracy. The original deck of computer cards used for calibration data contained only the points that correspond to the H_2O and CO_2 lines. Data for six calibration points were included on each card. In a few cases a complete new calibration card with six calibration points was added by including four or five interpolated points to complete a new card, the new card was inserted in the deck, making it possible to use original calibration cards that followed in the deck. The calibration point indicated by Ext in Table 4 was found by extrapolating with a second-order equation beyond the last CO_2 calibration line.

The combined calibration errors in the spectra are believed to be less than 0.1 cm^{-1}. With only one exception, all of the points corresponding to the H_2O and CO_2 calibration lines fell on a smooth curve of fiducial mark position vs wavenumber, indicating consistency among the points. The lone exception to this was the H_2O line centered at 504.45 cm^{-1}. This point would fit the smooth curve better if it were plotted at 504.35 cm^{-1}, approximately 0.1 cm^{-1} from the value commonly accepted as the line center. Although it seems unlikely, this apparent discontinuity in the calibration may be due to a faulty grating drive in the spectrometer. Because of this slight inconsistency in the calibration data, the wavenumber calibration may be less accurate between this 504.45 cm^{-1} H_2O line and either of the adjacent calibration lines than in the remainder of the spectral region.

RESULTS

The results of the CO_2 transmission measurements are presented in detail in the form of spectral plots of transmittance and tables of the cumulative integrated absorptance, $\int A\, d\nu$. ($A = 1-T$, where T is the experimentally observed transmittance.) Figures 1 through 6 show spectral plots of transmittance for Samples HR01 through HR22; these plots were obtained with either Resolution Schedule A or B. The caption of each figure includes the total pressure P, the equivalent pressure P_e, the absorber thickness u, and the temperature θ for each sample represented. Listings of the parameters occur in the same order, from top to bottom, as the corresponding spectral curves. Some of the sample parameters that are not listed in the figure captions are given in Table 1. The spectral plots of transmittance for samples HR23 through HR45 are presented in Figures 7 through 13. A few of the transmittance plots for a single sample extend over more than one panel in a figure. A short portion of each spectrum in these cases is represented by a dashed curve.

Tables 5 through 16 show detailed data on the cumulative integrated absorptance $\int A\, d\nu$. Each column represents a single sample with the important sample parameters listed at the top of the column. The lower limit of integration, ν', is the first value of ν listed in each table. The value tabulated for ν represents the value of the integral from ν' to ν. The value of the integral

between two values of ν that are listed is equal to the difference between the corresponding values of the integral. The data are of course, based on experimental curves obtained with finite spectral resolution; therefore, the integral values may differ from the true integrated absorptance that would be determined with infinite resolving power. Each of the separate tables represents the samples studied over a given spectral region.

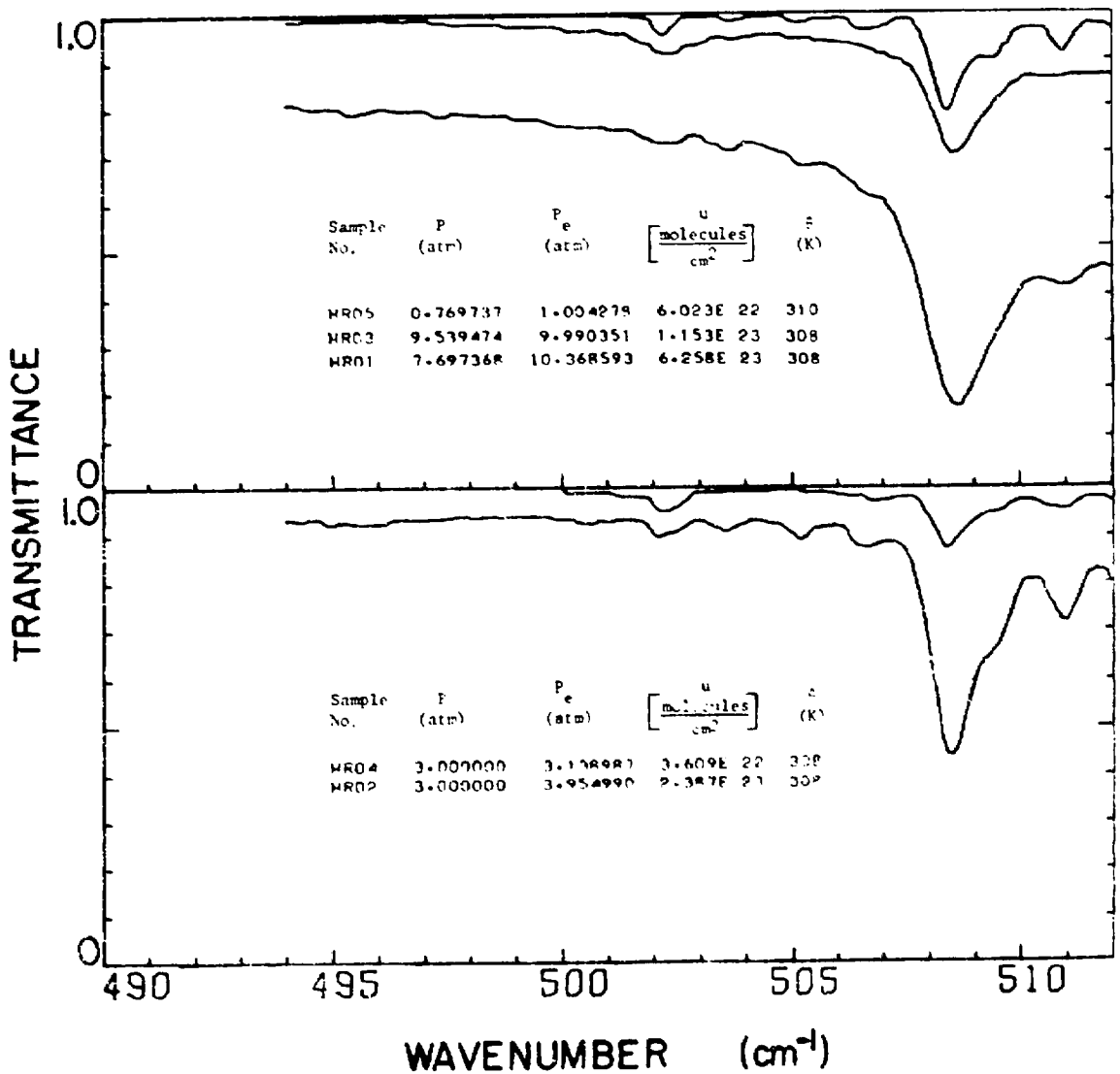

Figure 1. Spectral plots of transmittance from 494 to 512 cm^{-1} for Samples HR01 - HR05.

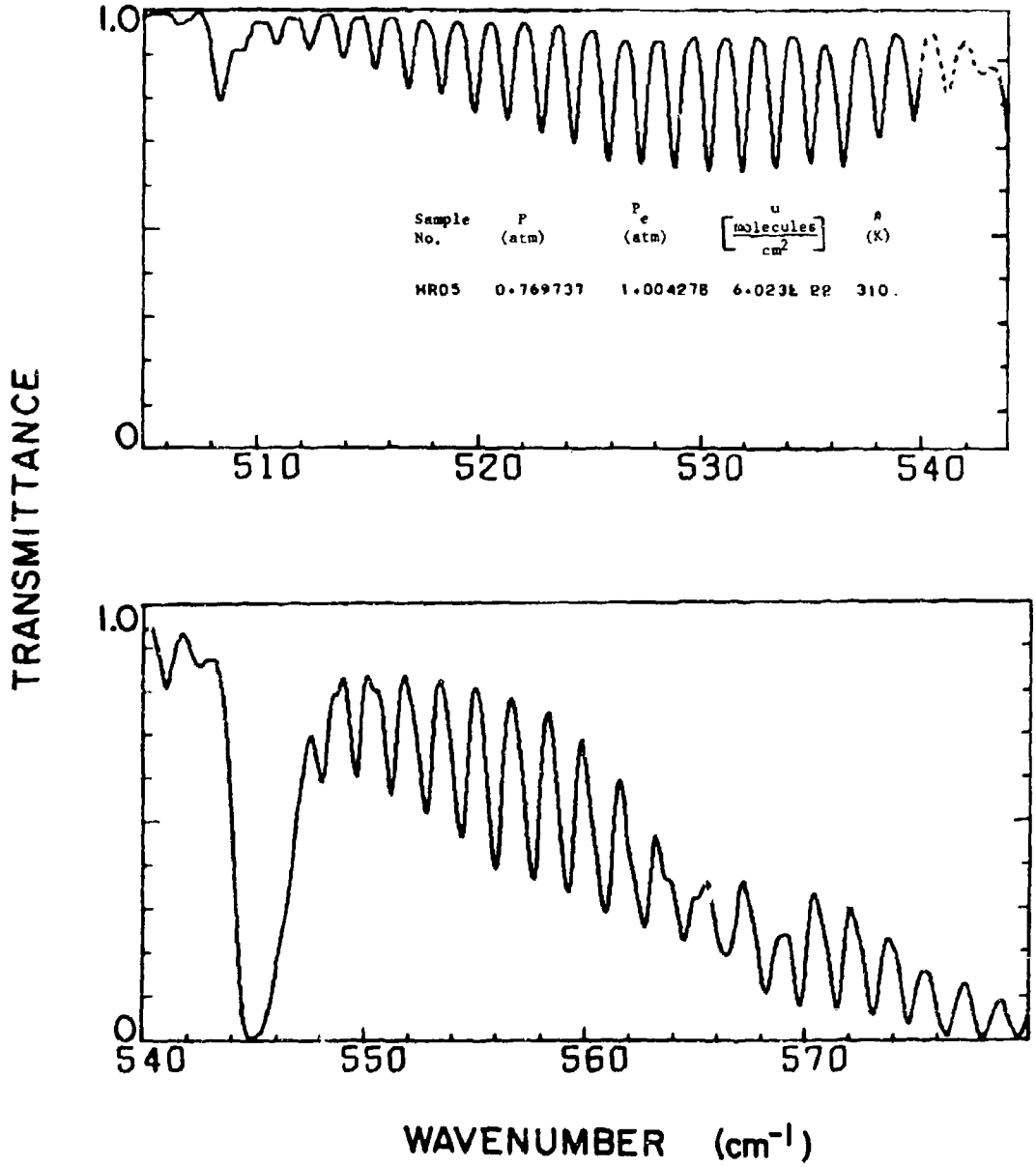

Figure 2. Spectral plot of transmittance from 505 to 580 cm^{-1} for Sample HR05.

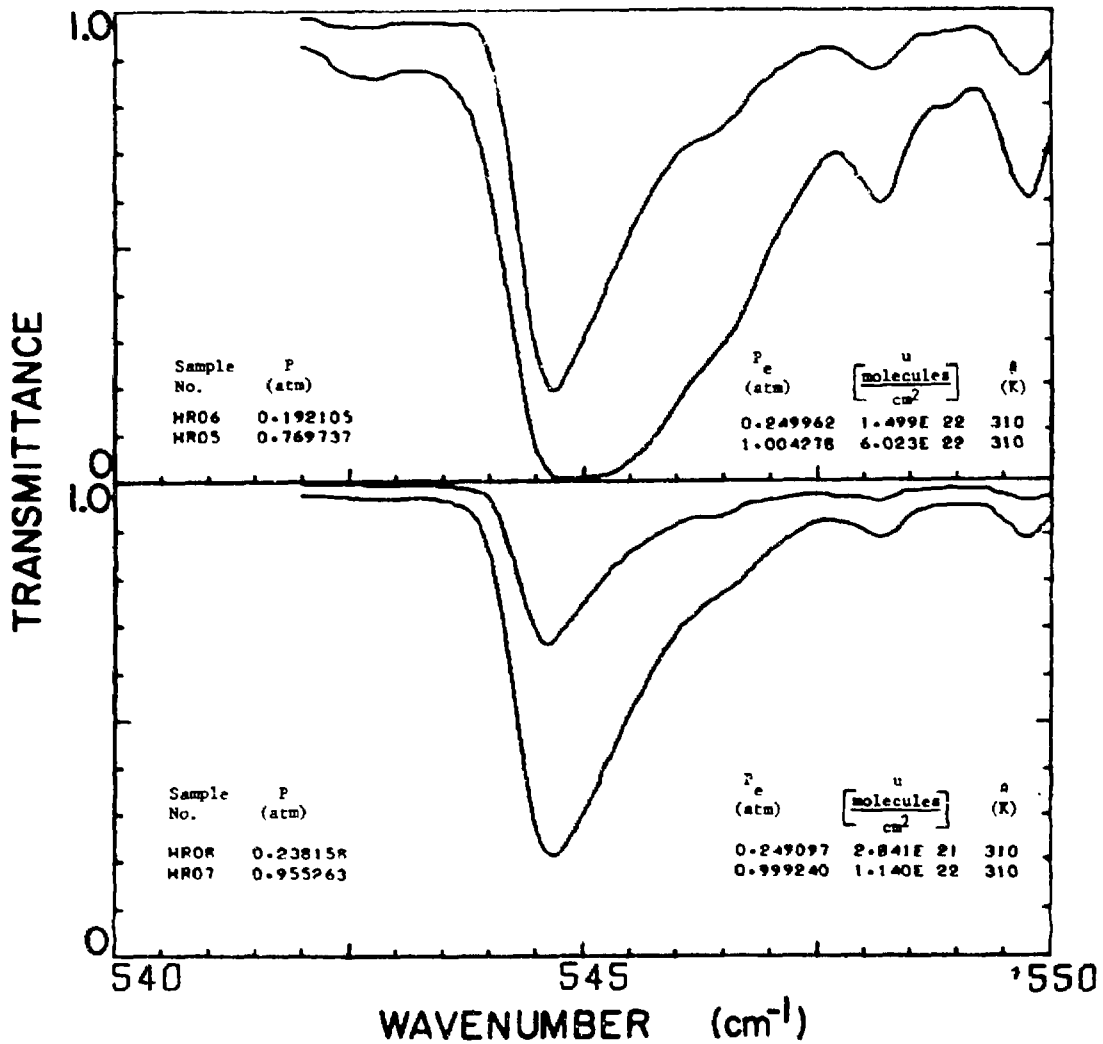

Figure 3. Spectral plots of transmittance from 542 to 550 cm^{-1} for Samples HR05 - HR08.

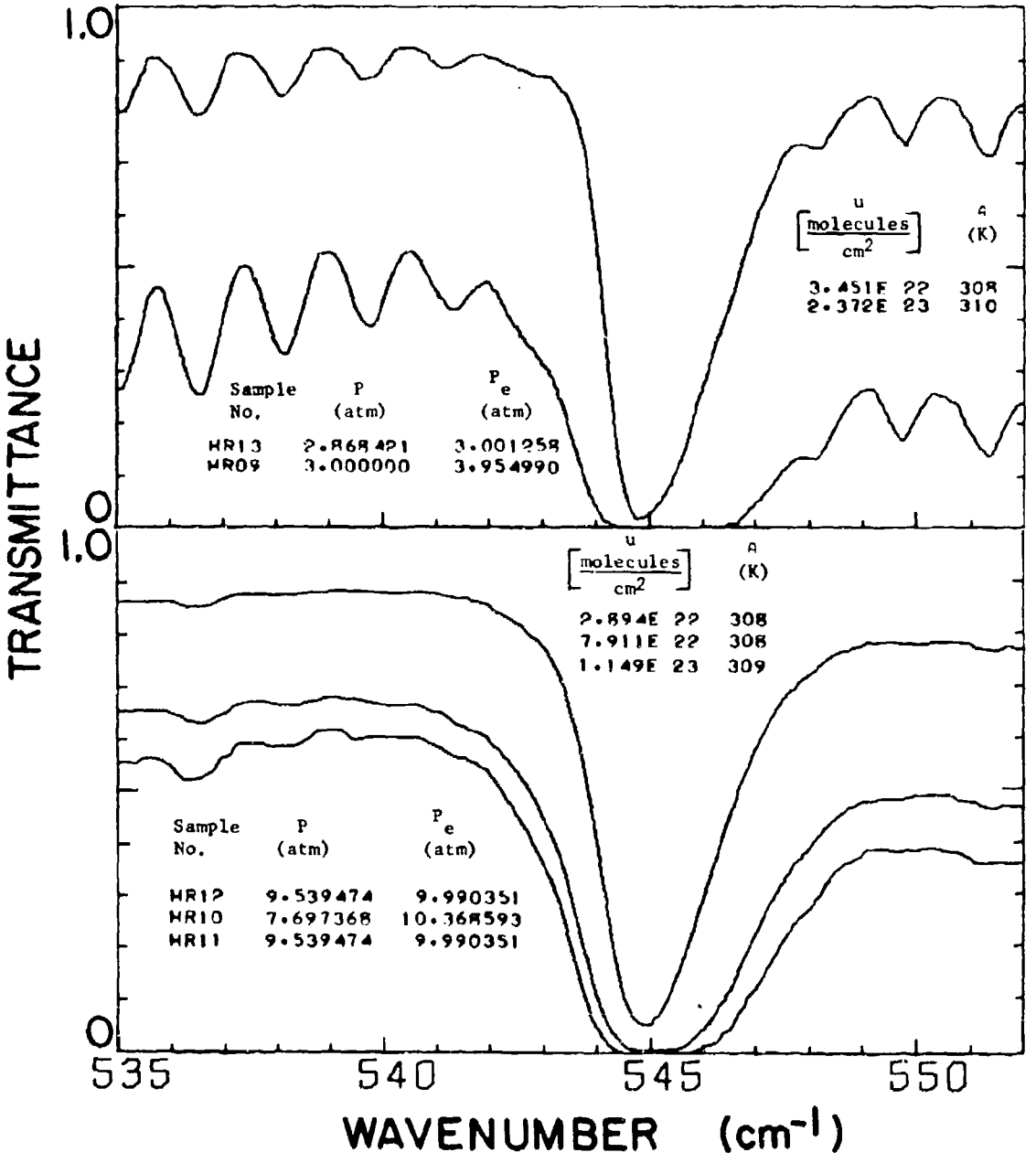

Figure 4. Spectral plots of transmittance from 535 to 552 cm^{-1} for Samples HR09 - HR13.

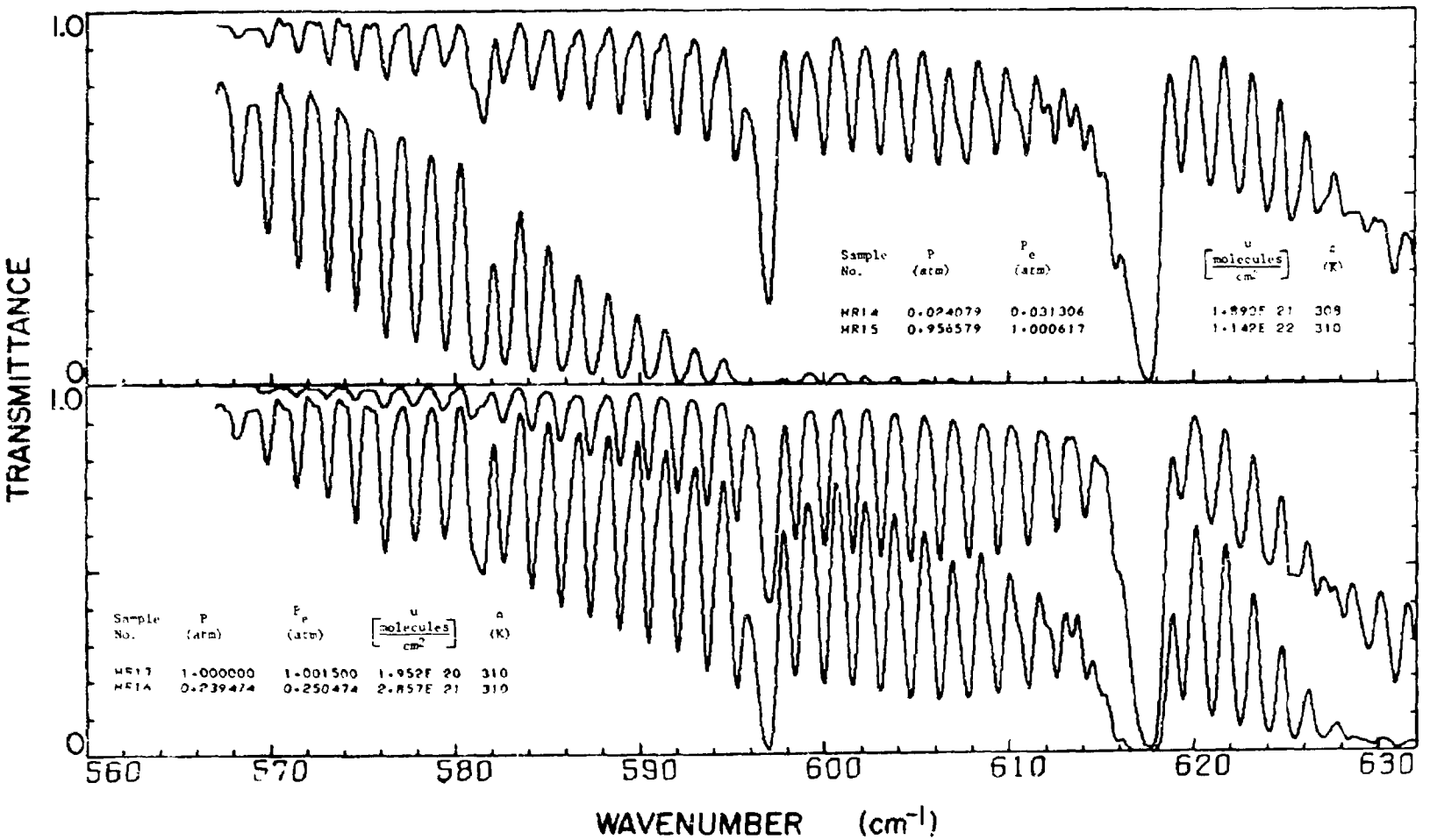

Figure 7. Spectral plots of transmittance from 567 to 632 cm^{-1} for Samples HR14 - HR17.

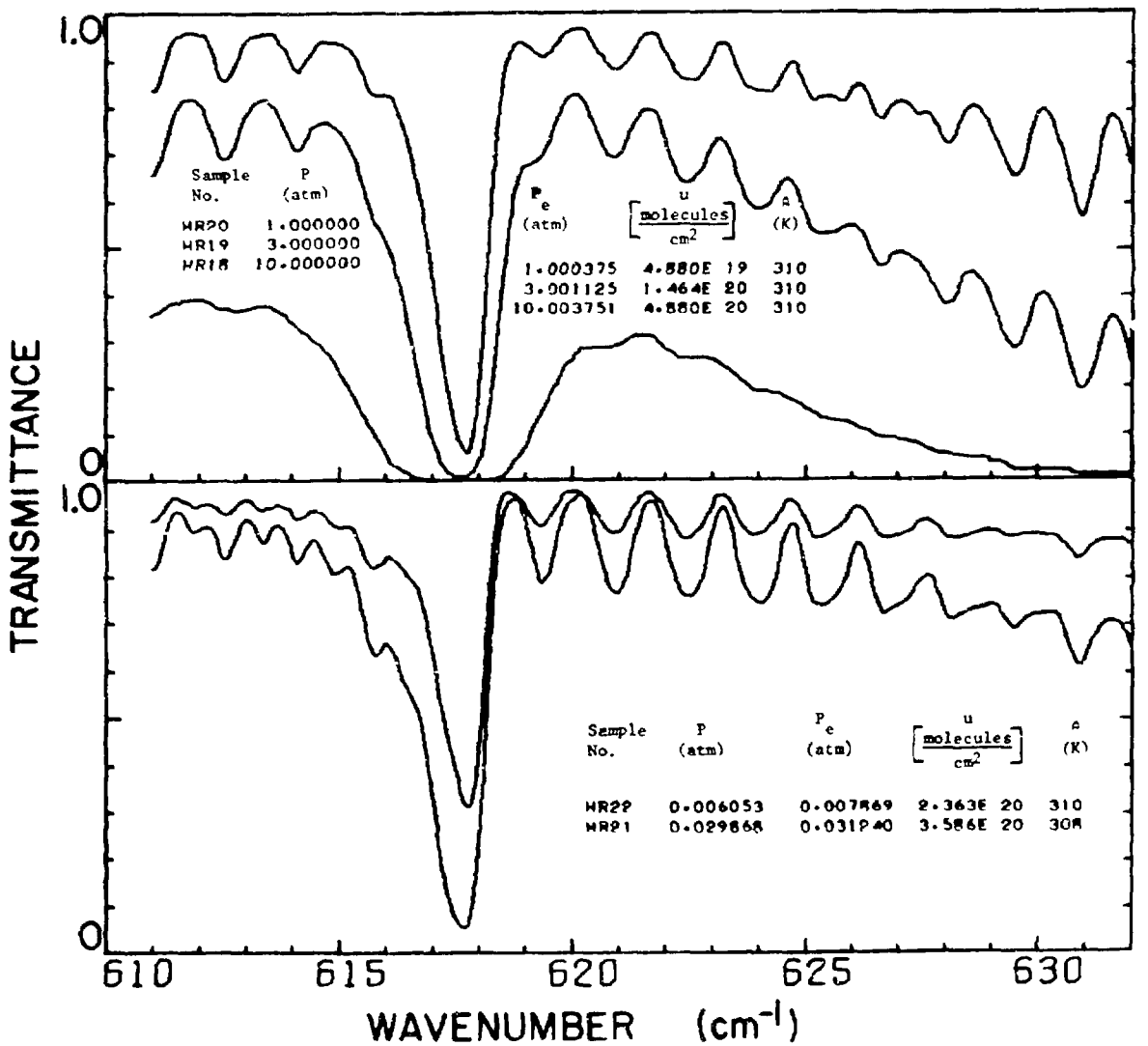

Figure 6. Spectral plots of transmittance from 611 to 632 cm^{-1} for Samples HR18 - HR22.

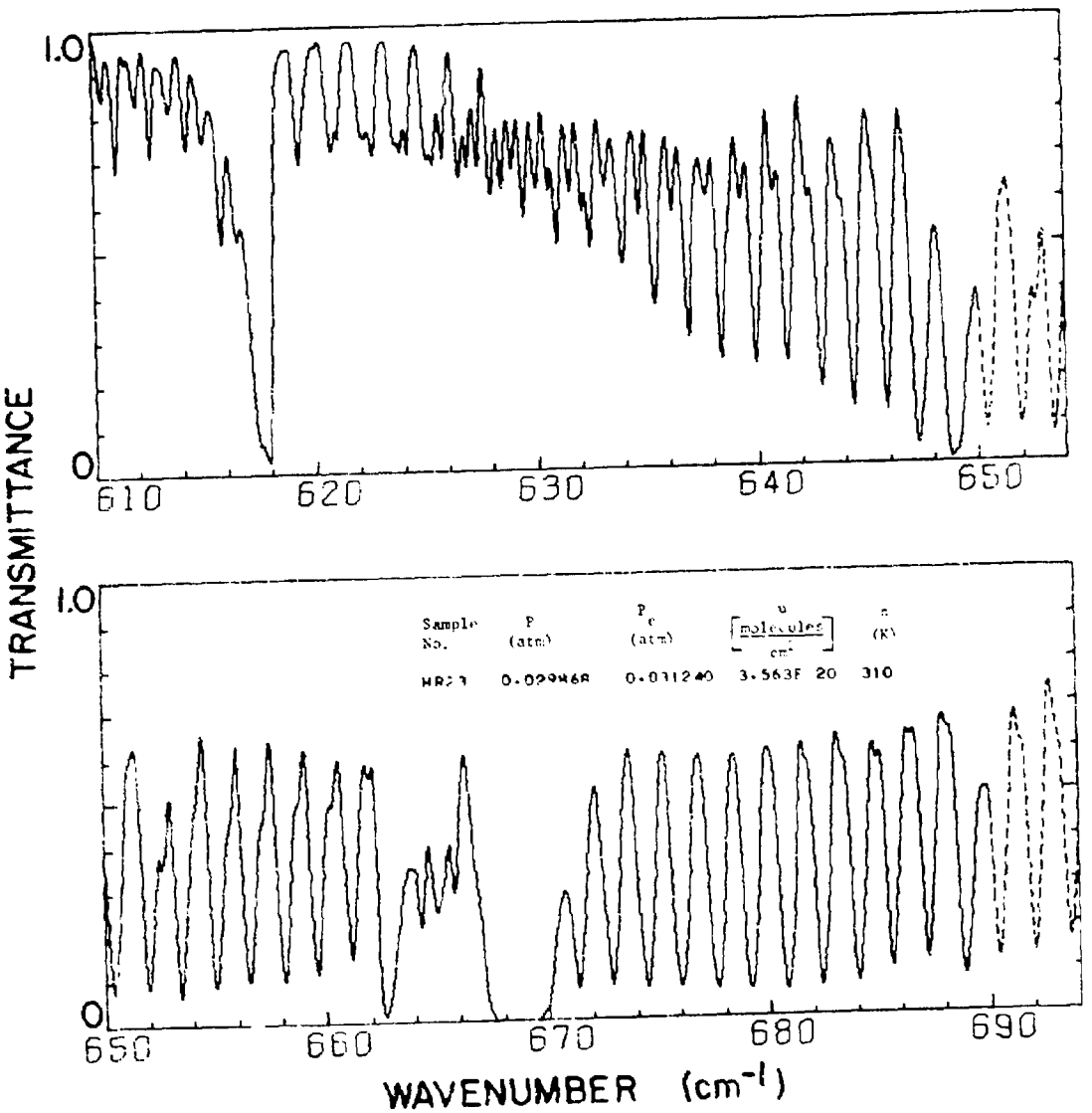

Figure 7. Spectral plot of transmittance from 610 to 694 cm^{-1} for Sample HR23.

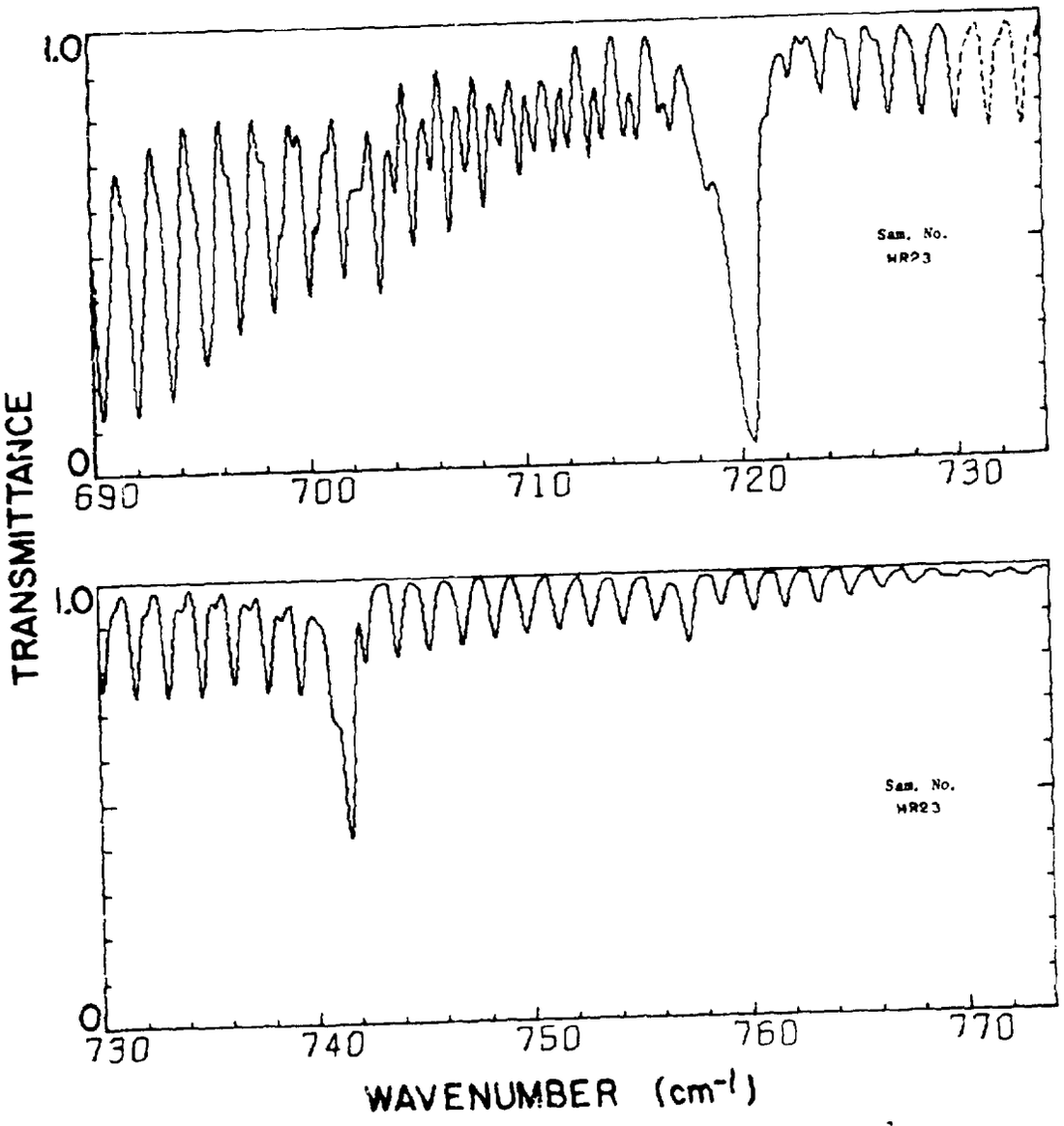

Figure 8. Spectral plot of transmittance from 690 to 775 cm^{-1} for Sample HR23.

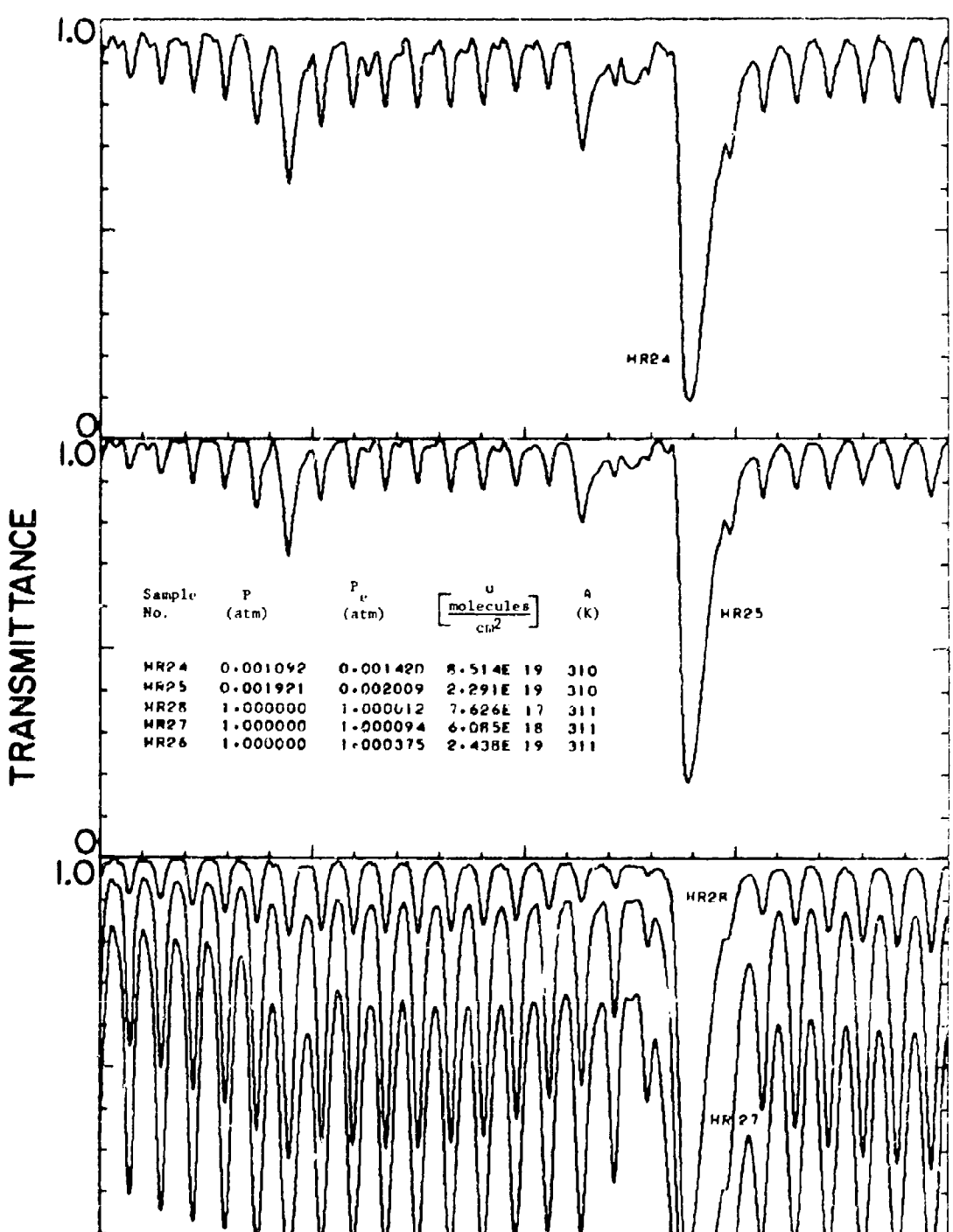

Sample No.	P (atm)	P_e (atm)	u $\left[\frac{\text{molecules}}{\text{cm}^2}\right]$	A (K)
HR24	0.001092	0.001420	8.514E 19	310
HR25	0.001921	0.002009	2.291E 19	310
HR28	1.000000	1.000012	7.626E 17	311
HR27	1.000000	1.000094	6.085E 18	311
HR26	1.000000	1.000375	2.438E 19	311

Figure 9. Spectral plots of transmittance from 640 to 680 cm^{-1} for Samples HR 24 - HR 28.

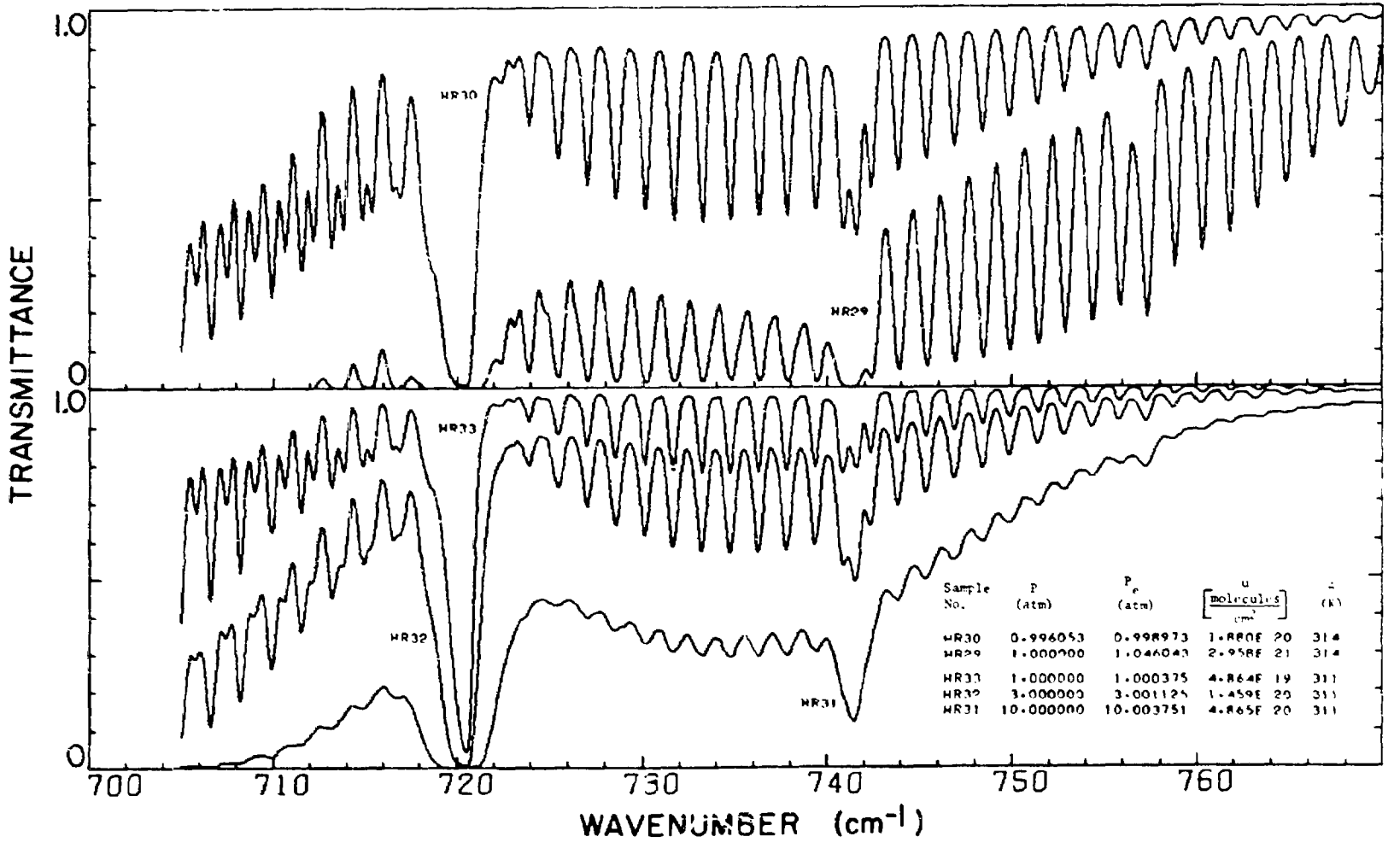

Figure 10. Spectral plots of transmittance from 705 to 770 cm^{-1} for Samples HR29 - HR33.

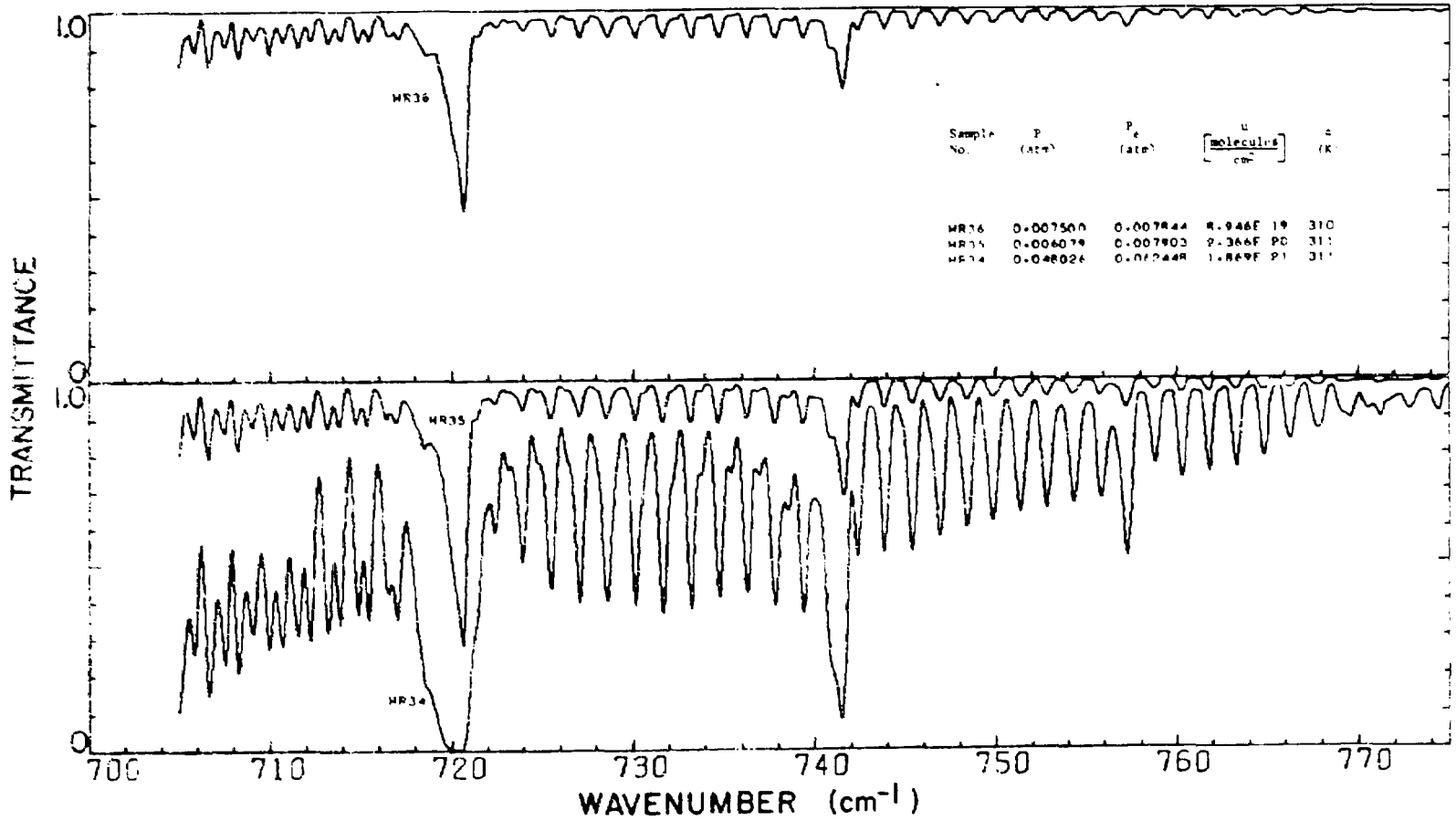

Figure 11. Spectral plots of transmittance from 705 to 775 cm^{-1} for Samples HR34 - HR36.

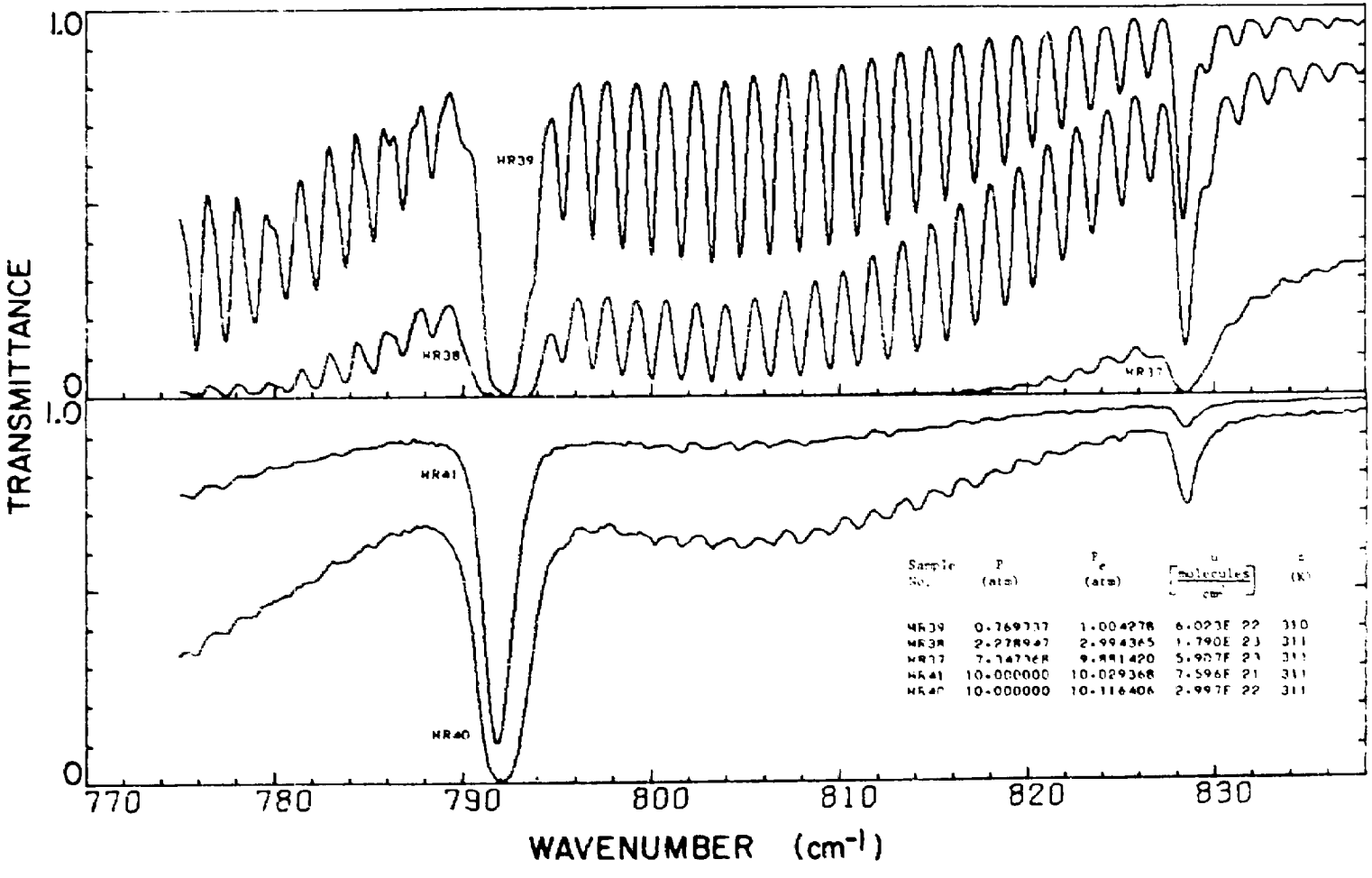

Figure 12. Spectral plots of transmittance from 775 to 838 cm^{-1} for Samples HR37 - HR41.

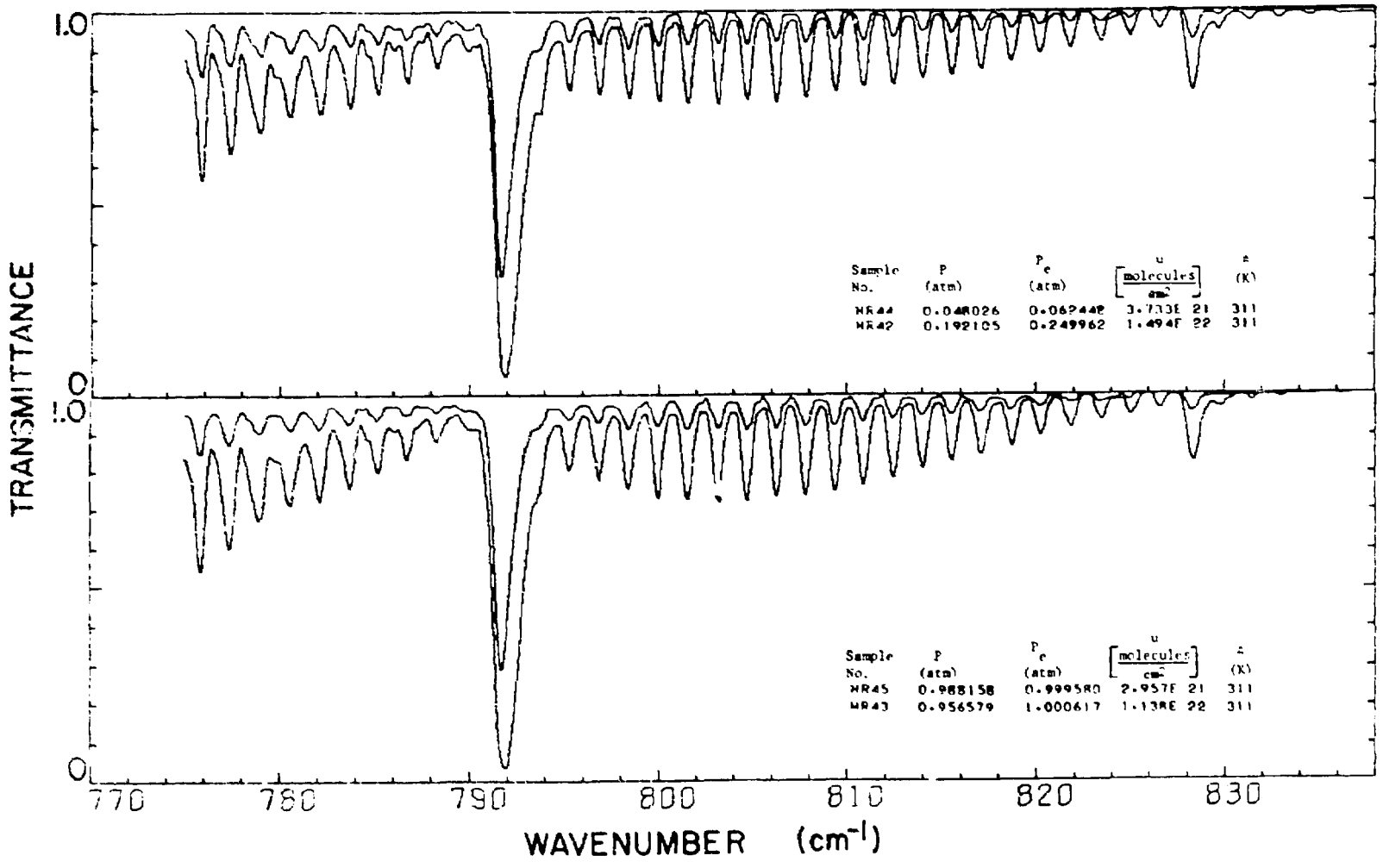

Figure 12. Spectral plots of transmittance from 775 - 838 cm^{-1} for Samples HR42 - HR45.

TABLE 5 $\int_{\nu'}^{\nu} A d\nu$

Sam. No.	HR01	HR02	HR03	HR04	HR05
Temp (K)	308.	308.	308.	308.	310.
Path (cm)	3291.	3291.	3291.	3291.	3291.
Conc.	1.00000	1.00000	0.15300	0.15300	1.00000
P (atm)	7.697368	3.000000	9.539474	3.000000	0.769737
P_e (atm)$_2$ *	10.368593	3.954990	9.990351	3.138987	1.004278
u_e (#/cm^2)	6.258E 23	2.387E 23	1.153E 23	3.609E 22	6.023E 22
ν (cm^{-1})					
494.00	0.	0.	0.	0.	0.
495.00	0.196	0.071	0.009	0.	0.
496.00	0.400	0.147	0.017	0.	0.
497.00	0.603	0.217	0.025	0.	0.
498.00	0.815	0.281	0.039	0.	0.
499.00	1.030	0.343	0.057	0.	0.
500.00	1.257	0.407	0.081	0.	0.
501.00	1.497	0.480	0.113	0.010	0.
502.00	1.749	0.555	0.161	0.027	0.005
503.00	2.016	0.644	0.234	0.064	0.023
504.00	2.295	0.728	0.285	0.074	0.026
505.00	2.581	0.808	0.328	0.082	0.032
506.00	2.902	0.901	0.379	0.091	0.041
507.00	3.272	1.016	0.446	0.113	0.065
508.00	3.779	1.189	0.561	0.143	0.092
509.00	4.565	1.681	0.824	0.246	0.246
510.00	5.236	1.999	1.010	0.298	0.319
511.00	5.804	2.226	1.142	0.334	0.363
512.00	6.351	2.433	1.271	0.364	0.392

* The units of u are molecules/cm^2, abbreviated here by (#/cm^2).

TABLE 6 $\int A d\nu$

Sam. No.	HR05
Temp (K)	310.
Path (cm)	3291.
Conc.	1.00000
P (atm)	0.769737
P_e (atm)	1.004278
u (#/cm^2)*	6.023E 22

ν (cm^{-1})	
505.00	0.
506.00	0.010
507.00	0.033
508.00	0.060
509.00	0.215
510.00	0.287
511.00	0.332
512.00	0.360
513.00	0.415
514.00	0.463
515.00	0.495
516.00	0.570
517.00	0.654
518.00	0.701
519.00	0.809
520.00	0.927
521.00	0.989
522.00	1.135
523.00	1.270
524.00	1.350
525.00	1.526
526.00	1.700
527.00	1.816
528.00	2.034
529.00	2.223
530.00	2.335
531.00	2.564
532.00	2.735
533.00	2.861
534.00	3.097
535.00	3.231
536.00	3.399
537.00	3.643
538.00	3.754
539.00	3.908
540.00	4.066
541.00	4.147
542.00	4.276
543.00	4.397
544.00	4.575

Sam. No.	HR05
Temp (K)	310.
Path (cm)	3291.
Conc.	1.00000
p (atm)	0.769737
P (atm)	1.004278
u (#/cm^2)*	6.023E 22

ν (cm^{-1})	
545.00	5.406
546.00	6.348
547.00	7.038
548.00	7.407
549.00	7.700
550.00	7.978
551.00	8.181
552.00	8.488
553.00	8.804
554.00	9.074
555.00	9.494
556.00	9.827
557.00	10.199
558.00	10.689
559.00	11.035
560.00	11.552
561.00	12.095
562.00	12.610
563.00	13.280
564.00	13.879
565.00	14.598
566.00	15.272
567.00	16.048
568.00	16.756
569.00	17.590
570.00	18.422
571.00	19.149
572.00	20.000
573.00	20.786
574.00	21.629
575.00	22.526
576.00	23.394
577.00	24.346
578.00	25.271
579.00	26.215
580.00	27.187

* The units of u are molecules/cm^2, abbreviated here by (#/cm^2).

TABLE 7 $\int_{\nu'}^{\nu} A d\nu$

Sam. No.	HR05	HR06	HR07	HR08
Temp (K)	310.	310.	310.	310.
Path (cm)	3291.	3291.	3291.	3291.
Conc.	1.00000	1.00000	0.15300	0.15300
P (atm)	0.769737	0.192105	0.955263	0.238158
P_e (atm)$_2$	1.004278	0.249962	0.999240	0.249097
u^e (#/cm^2)*	6.023E 22	1.499E 22	1.140E 22	2.841E 21
ν (cm^{-1})				
542.00	0.	0.	0.	0.
543.00	0.121	0.026	0.031	0.002
544.00	0.299	0.055	0.083	0.010
545.00	1.131	0.639	0.683	0.248
546.00	2.072	1.126	1.174	0.403
547.00	2.762	1.363	1.398	0.464
548.00	3.131	1.463	1.492	0.491
549.00	3.425	1.545	1.568	0.511
550.00	3.703	1.631	1.643	0.533

* The units of u are molecules/cm^2, abbreviated here by (#/cm^2).

TABLE 8 $\int_{\nu'}^{\nu} A\,d\nu$

Sam. No.	HR09	HR10	HR11	HR12	HR13
Temp (K)	310.	308.	309.	308.	308.
Path (cm)	3291.	416.	3291.	826.	3291.
Conc.	1.00000	1.00000	0.15300	0.15300	0.15300
P (atm)	3.000000	7.697368	9.539474	9.539474	2.868421
P_e (atm)	3.954990	10.368593	9.990351	9.990351	3.001258
u (#/cm^2)*	2.372E 23	7.911E 22	1.149E 23	2.894E 22	3.451E 22
ν (cm^{-1})					
535.00	0.	0.	0.	0.	0.
536.00	0.621	0.344	0.441	0.133	0.140
537.00	1.308	0.704	0.907	0.274	0.315
538.00	1.857	1.035	1.320	0.393	0.424
539.00	2.429	1.361	1.719	0.509	0.548
540.00	2.987	1.687	2.111	0.624	0.664
541.00	3.492	2.025	2.507	0.740	0.754
542.00	4.051	2.401	2.943	0.872	0.860
543.00	4.666	2.871	3.490	1.053	0.976
544.00	5.483	3.580	4.281	1.420	1.189
545.00	6.478	4.552	5.272	2.267	2.024
546.00	7.478	5.536	6.270	3.111	2.907
547.00	8.467	6.407	7.217	3.658	3.485
548.00	9.365	7.081	8.010	3.985	3.796
549.00	10.171	7.632	8.672	4.221	4.025
550.00	10.956	8.142	9.282	4.433	4.243
551.00	11.722	8.649	9.894	4.644	4.437
552.00	12.541	9.175	10.528	4.867	4.682

* The units of u are molecules/cm^2, abbreviated here by (#/cm^2).

TABLE 9 $\int_{\nu'}^{\nu} A d\nu$

Sam. No.	HR14	HR15	HR16	HR17
Temp (K)	308.	310.	310.	310.
Path (cm)	3291.	3291.	3291.	1648.
Conc.	1.00000	0.15300	0.15300	0.00500
P (atm)	0.024079	0.956579	0.239474	1.000000
P_e (atm)	0.031306	1.000617	0.250474	1.001500
u (#/cm^2) *	1.890E 21	1.142E 22	2.857E 21	1.952E 20
ν (cm^{-1})				
567.00	0.	0.	0.	0.
568.00	0.042	0.258	0.070	0.
569.00	0.100	0.619	0.179	0.
570.00	0.166	1.040	0.308	0.014
571.00	0.202	1.308	0.374	0.024
572.00	0.276	1.800	0.542	0.042
573.00	0.321	2.149	0.629	0.058
574.00	0.389	2.585	0.765	0.077
575.00	0.480	3.154	0.973	0.103
576.00	0.530	3.554	1.075	0.124
577.00	0.643	4.196	1.336	0.162
578.00	0.736	4.802	1.552	0.198
579.00	0.803	5.343	1.703	0.218
580.00	0.915	6.111	1.995	0.268
581.00	1.015	6.732	2.187	0.307
582.00	1.255	7.624	2.626	0.367
583.00	1.396	8.465	2.968	0.435
584.00	1.470	9.143	3.156	0.470
585.00	1.615	9.997	3.510	0.541
586.00	1.765	10.842	3.883	0.631
587.00	1.851	11.642	4.119	0.680
588.00	2.033	12.577	4.578	0.807
589.00	2.167	13.436	4.923	0.905
590.00	2.283	14.339	5.242	0.981
591.00	2.473	15.294	5.739	1.137
592.00	2.623	16.202	6.096	1.240
593.00	2.794	17.162	6.532	1.372
594.00	3.035	18.133	7.096	1.579
595.00	3.202	19.094	7.500	1.682
596.00	3.529	20.093	8.206	1.917
597.00	4.083	21.093	9.074	2.273
598.00	4.470	22.088	9.731	2.611
599.00	4.714	23.082	10.342	2.884
600.00	4.941	24.070	10.881	3.079
601.00	5.112	25.055	11.340	3.262

* The units of u are molecules/cm^2, abbreviated here by (#/cm^2).

TABLE 9 $\int_{\nu'}^{\nu} A d\nu$ (cont.)

Sam. No.	HR14	HR15	HR16	HR17
Temp (K)	308.	310.	310.	310.
Path (cm)	3291.	3291.	3291.	1648.
Conc.	1.00000	0.15300	0.15300	0.00500
P (atm)	0.024079	0.956579	0.239474	1.000000
P_e (atm)	0.031306	1.000617	0.250474	1.001500
u (#/cm^2)*	1.890E 21	1.142E 22	2.857E 21	1.952E 20
ν (cm^{-1})				
602.00	5.375	26.051	12.002	3.556
603.00	5.572	27.046	12.537	3.746
604.00	5.783	28.040	13.092	3.966
605.00	6.094	29.039	13.820	4.293
606.00	6.282	30.037	14.360	4.455
607.00	6.567	31.034	15.054	4.752
608.00	6.912	32.034	15.794	5.055
609.00	7.119	33.034	16.377	5.225
610.00	7.403	34.034	17.101	5.550
611.00	7.688	35.034	17.768	5.783
612.00	7.941	36.034	18.434	6.010
613.00	8.231	37.034	19.154	6.300
614.00	8.514	38.034	19.822	6.498
615.00	8.887	39.034	20.620	6.764
616.00	9.460	40.034	21.536	7.149
617.00	10.234	41.034	22.527	7.875
618.00	11.201	42.034	23.527	8.851
619.00	11.564	43.034	24.323	9.315
620.00	11.880	44.034	25.036	9.554
621.00	12.173	45.034	25.679	9.790
622.00	12.430	46.034	26.307	10.018
623.00	12.846	47.034	27.149	10.409
624.00	13.182	48.034	27.895	10.749
625.00	13.573	49.034	28.727	11.162
626.00	14.064	50.034	29.661	11.678
627.00	14.539	51.034	30.567	12.192
628.00	15.027	52.034	31.514	12.759
629.00	15.576	53.034	32.485	13.356
630.00	16.154	54.034	33.467	14.039
631.00	16.780	55.034	34.449	14.717
632.00	17.412	56.034	35.434	15.395

* The units of u are molecules/cm^2, abbreviated here by (#/cm^2).

TABLE 10 $\int_{\nu'}^{\nu} A d\nu$

Sam. No.	HR18	HR19	HR20	HR21	HR22
Temp (K)	310.	310.	310.	308.	310.
Path (cm)	1648.	1648.	1648.	3291.	1648.
Conc.	0.00125	0.00125	0.00125	0.15300	1.00000
P (atm)	10.000000	3.000000	1.000000	0.029868	0.006053
P_e (atm)	10.003751	3.001125	1.000375	0.031240	0.007869
u_ν (#/cm^2) *	4.880E 20	1.464E 20	4.880E 19	3.586E 20	2.363E 20
(cm^{-1})					
611.00	0.	0.	0.	0.	0.
612.00	0.621	0.235	0.074	0.105	0.050
613.00	1.248	0.500	0.171	0.224	0.102
614.00	1.884	0.712	0.229	0.330	0.155
615.00	2.592	0.967	0.310	0.488	0.230
616.00	3.452	1.336	0.438	0.763	0.372
617.00	4.437	2.023	0.752	1.220	0.591
618.00	5.437	2.998	1.587	2.082	1.165
619.00	6.415	3.605	1.846	2.289	1.300
620.00	7.236	3.868	1.915	2.423	1.361
621.00	7.952	4.111	1.990	2.545	1.423
622.00	8.649	4.349	2.061	2.653	1.473
623.00	9.383	4.683	2.187	2.853	1.569
624.00	10.161	5.020	2.301	3.004	1.636
625.00	10.984	5.409	2.443	3.175	1.708
626.00	11.853	5.872	2.624	3.411	1.810
627.00	12.755	6.378	2.815	3.629	1.902
628.00	13.685	6.928	3.035	3.861	1.999
629.00	14.638	7.513	3.268	4.137	2.115
630.00	15.612	8.186	3.569	4.427	2.227
631.00	16.595	8.877	3.870	4.747	2.358
632.00	17.584	9.585	4.161	5.065	2.489

* The units of u are molecules/cm^2, abbreviated here by (#/cm^2).

TABLE II $\int_{\nu'}^{\nu} A d\nu$

Sam. No.	HR23	Sam. No.	HR23	Sam. No.	HR23
Temp (K)	310.	Temp (K)	310.	Temp (K)	310.
Path (cm)	3291.	Path (cm)	3291.	Path (cm)	3291.
Conc.	0.15300	Conc.	0.15300	Conc.	0.15300
P (atm)	0.029868	p (atm)	0.029868	p (atm)	0.029868
P_e (atm)	0.031240	P (atm)	0.031240	P (atm)	0.031240
u^2 (#/cm^2)*	3.563E 20	u_2 (#/cm^2)*	3.563E 20	u (#/cm^2)*	3.563E 20
ν (cm^{-1})		ν (cm^{-1})		ν (cm^{-1})	
610.00	0.	665.00	24.182	720.00	51.654
611.00	0.113	666.00	24.852	721.00	52.495
612.00	0.234	667.00	25.407	722.00	52.672
613.00	0.365	668.00	26.370	723.00	52.759
614.00	0.480	669.00	27.370	724.00	52.853
615.00	0.661	670.00	28.362	725.00	52.913
616.00	0.955	671.00	29.154	726.00	53.037
617.00	1.399	672.00	29.922	727.00	53.120
618.00	2.293	673.00	30.617	728.00	53.214
619.00	2.474	674.00	31.181	729.00	53.355
620.00	2.636	675.00	31.970	730.00	53.418
621.00	2.777	676.00	32.588	731.00	53.536
622.00	2.881	677.00	33.215	732.00	53.669
623.00	3.101	678.00	34.002	733.00	53.728
624.00	3.263	679.00	34.552	734.00	53.854
625.00	3.422	680.00	35.249	735.00	53.976
626.00	3.690	681.00	35.956	736.00	54.026
627.00	3.912	682.00	36.462	737.00	54.148
628.00	4.146	683.00	37.232	738.00	54.271
629.00	4.438	684.00	37.785	739.00	54.351
630.00	4.741	685.00	38.388	740.00	54.503
631.00	5.075	686.00	39.064	741.00	54.693
632.00	5.384	687.00	39.507	742.00	55.099
633.00	5.746	688.00	40.132	743.00	55.193
634.00	6.129	689.00	40.720	744.00	55.265

TABLE II (Cont'd.)

635.00	6.463	690.00	41.330	745.00	55.295
636.00	6.898	691.00	42.026	746.00	55.379
637.00	7.552	692.00	42.500	747.00	55.444
638.00	7.727	693.00	43.028	748.00	55.476
639.00	8.235	694.00	43.644	749.00	55.553
640.00	8.693	695.00	43.994	750.00	55.613
641.00	9.090	696.00	44.563	751.00	55.644
642.00	9.593	697.00	45.003	752.00	55.720
643.00	10.091	698.00	45.347	753.00	55.775
644.00	10.508	699.00	45.828	754.00	55.805
645.00	11.095	700.00	46.130	755.00	55.870
646.00	11.616	701.00	46.553	756.00	55.921
647.00	12.015	702.00	46.928	757.00	55.966
648.00	12.804	703.00	47.258	758.00	56.049
649.00	13.566	704.00	47.671	759.00	56.086
650.00	14.341	705.00	47.982	760.00	56.103
651.00	15.096	706.00	48.268	761.00	56.146
652.00	15.655	707.00	48.540	762.00	56.185
653.00	16.318	708.00	48.763	763.00	56.199
654.00	17.059	709.00	49.038	764.00	56.237
655.00	17.618	710.00	49.262	765.00	56.266
656.00	18.251	711.00	49.480	766.00	56.279
657.00	18.965	712.00	49.682	767.00	56.307
658.00	19.505	713.00	49.845	768.00	56.331
659.00	20.153	714.00	50.074	769.00	56.345
660.00	20.832	715.00	50.212	770.00	56.369
661.00	21.352	716.00	50.359	771.00	56.388
662.00	21.964	717.00	50.541	772.00	56.409
663.00	22.754	718.00	50.700	773.00	56.428
664.00	23.483	719.00	51.049	774.00	56.440
				775.00	56.455

* The units of u are molecules/cm^2, abbreviated here by (#/cm^2).

TABLE 12 $\int_{\nu'} A d\nu$

Sam. No.	HR24	HR25	HR26	HR27	HR28
Temp (K)	310.	310.	311.	311.	311.
Path (cm)	3291.	3291.	826.	826.	826.
Conc.	1.00000	0.15300	0.00125	0.000312	0.000039
P (atm)	0.001092	0.001921	1.000000	1.000000	1.000000
P_e (atm)	0.001420	0.002009	1.000375	1.000094	1.000012
u^e (#/cm^2) *	8.514E 19	2.291E 19	2.438E 19	6.085E 18	7.626E 17
ν (cm^{-1})					
640.00	0.	0.	0.	0.	0.
641.00	0.057	0.016	0.290	0.108	0.017
642.00	0.138	0.051	0.797	0.341	0.057
643.00	0.218	0.085	1.235	0.543	0.095
644.00	0.276	0.098	1.570	0.671	0.110
645.00	0.365	0.136	2.145	0.959	0.163
646.00	0.449	0.173	2.634	1.201	0.207
647.00	0.508	0.186	3.026	1.357	0.229
648.00	0.662	0.272	3.722	1.727	0.300
649.00	0.867	0.398	4.375	2.084	0.373
650.00	1.034	0.476	4.964	2.341	0.413
651.00	1.180	0.544	5.673	2.732	0.496
652.00	1.278	0.579	6.216	3.010	0.552
653.00	1.389	0.603	6.750	3.249	0.593
654.00	1.512	0.649	7.473	3.658	0.676
655.00	1.605	0.673	8.030	3.911	0.725
656.00	1.694	0.696	8.593	4.192	0.773
657.00	1.809	0.746	9.331	4.591	0.858
658.00	1.887	0.772	9.853	4.803	0.894
659.00	1.982	0.814	10.455	5.118	0.955
660.00	2.080	0.867	11.141	5.482	1.026
661.00	2.146	0.891	11.598	5.647	1.050
662.00	2.235	0.931	12.180	5.942	1.103
663.00	2.433	1.050	12.827	6.251	1.155
664.00	2.577	1.119	13.240	6.387	1.175
665.00	2.704	1.181	13.764	6.601	1.209
666.00	2.832	1.232	14.189	6.738	1.231
667.00	2.901	1.247	14.783	6.968	1.273
668.00	3.501	1.771	15.764	7.854	1.940
669.00	4.164	2.306	16.758	8.836	2.552
670.00	4.489	2.525	17.741	9.618	2.751
671.00	4.625	2.596	18.491	9.945	2.803
672.00	4.766	2.669	19.207	10.315	2.875
673.00	4.878	2.720	19.875	10.653	2.947
674.00	4.955	2.744	20.402	10.863	2.981
675.00	5.081	2.804	21.190	11.302	3.077
676.00	5.162	2.834	21.797	11.591	3.139
677.00	5.254	2.871	22.433	11.912	3.204
678.00	5.377	2.935	23.226	12.382	3.313
679.00	5.440	2.957	23.784	12.608	3.351
680.00	5.558	3.021	24.530	13.037	3.451

* The units of u are molecules/cm^2, abbreviated here by (#/cm^2).

TABLE 13 $\int A d\nu$

Sam. No.	HR29	HR30	HR31	HR32	HR33
Temp (K)	314.	314.	311.	311.	311.
Path (cm)	826.	826.	1648.	1648.	1648.
Conc.	0.15300	0.00977	0.00125	0.00125	0.00125
P (atm)	1.000000	0.996053	10.000000	3.000000	1.000000
P_e (atm)	1.046043	0.998973	10.003751	3.001125	1.000375
u (#/cm^2) *	2.958E 21	1.880E 20	4.865E 20	1.459E 20	4.864E 19
ν (cm^{-1})					
705.00	0.	0.	0.	0.	0.
706.00	1.000	0.707	0.994	0.755	0.325
707.00	2.000	1.410	1.989	1.539	0.679
708.00	3.000	2.017	2.975	2.185	0.918
709.00	4.000	2.680	3.954	2.877	1.228
710.00	5.000	3.277	4.922	3.494	1.479
711.00	6.000	3.836	5.872	4.052	1.691
712.00	7.000	4.372	6.806	4.606	1.901
713.00	7.988	4.807	7.703	5.041	2.050
714.00	8.985	5.351	8.581	5.528	2.254
715.00	9.951	5.712	9.421	5.891	2.370
716.00	10.914	6.092	10.231	6.244	2.495
717.00	11.894	6.501	11.036	6.597	2.625
718.00	12.875	6.821	11.878	6.912	2.716
719.00	13.873	7.471	12.834	7.488	2.958
720.00	14.873	8.399	13.833	8.385	3.533
721.00	15.873	9.353	14.832	9.362	4.387
722.00	16.849	9.715	15.792	9.840	4.518
723.00	17.737	9.885	16.544	10.017	4.556
724.00	18.613	10.084	17.158	10.183	4.604
725.00	19.419	10.229	17.718	10.326	4.637
726.00	20.312	10.492	18.284	10.535	4.711
727.00	21.158	10.702	18.860	10.721	4.766
728.00	21.992	10.911	19.454	10.918	4.823
729.00	22.929	11.248	20.083	11.194	4.931
730.00	23.756	11.434	20.715	11.398	4.981
731.00	24.653	11.728	21.370	11.656	5.073
732.00	25.570	12.074	22.046	11.965	5.193
733.00	26.418	12.260	22.715	12.186	5.242
734.00	27.337	12.580	23.397	12.479	5.351
735.00	28.242	12.919	24.086	12.792	5.469
736.00	29.095	13.095	24.7[illegible]	13.007	5.516
737.00	30.01[illegible]	13.425	25.457	13.306	5.628
738.00	30.921	13.744	26.117	13.605	5.741
739.00	31.799	13.933	26.774	13.816	5.788

* The units of u are molecules/cm^2, abbreviated here by (#/cm^2).

TABLE 13 $\int_{\nu'}^{\nu} A d\nu$ (cont.)

Sam. No.	HR29	HR30	HR31	HR32	HR33
Temp (K)	314.	314.	311.	311.	311.
Path (cm)	826.	826.	1648.	1648.	1648.
Conc.	0.15300	0.00977	0.00125	0.00125	0.00125
P (atm)	1.000000	0.996053	10.000000	3.000000	1.000000
P_e(atm)	1.046043	0.998973	10.003751	3.001125	1.000375
u(#/cm^2)*	2.958E 21	1.880E 20	4.865E 20	1.459E 20	4.864E 19
ν (cm^{-1})					
740.00	32.741	14.275	27.455	14.122	5.902
741.00	33.695	14.629	28.193	14.442	6.021
742.00	34.683	15.124	29.038	14.887	6.186
743.00	35.560	15.420	29.682	15.151	6.281
744.00	36.325	15.649	30.228	15.354	6.352
745.00	36.991	15.778	30.719	15.491	6.381
746.00	37.792	16.022	31.198	15.687	6.453
747.00	38.498	16.207	31.634	15.840	6.504
748.00	39.110	16.329	32.036	15.951	6.532
749.00	39.874	16.532	32.422	16.102	6.585
750.00	40.528	16.691	32.767	16.217	6.624
751.00	41.073	16.787	33.078	16.300	6.643
752.00	41.788	16.952	33.374	16.410	6.682
753.00	42.367	17.075	33.634	16.494	6.708
754.00	42.843	17.157	33.866	16.556	6.720
755.00	43.476	17.284	34.086	16.634	6.746
756.00	43.989	17.380	34.281	16.694	6.764
757.00	44.476	17.452	34.472	16.744	6.777
758.00	45.049	17.559	34.656	16.807	6.798
759.00	45.485	17.636	34.793	16.850	6.810
760.00	45.752	17.683	34.909	16.878	6.814
761.00	46.167	17.752	35.017	16.912	6.825
762.00	46.521	17.811	35.112	16.941	6.832
763.00	46.709	17.849	35.194	16.961	6.835
764.00	47.047	17.904	35.273	16.987	6.843
765.00	47.313	17.948	35.344	17.007	6.847
766.00	47.478	17.979	35.407	17.024	6.849
767.00	47.743	18.020	35.466	17.042	6.853
768.00	47.954	18.054	35.520	17.058	6.856
769.00	48.102	18.082	35.569	17.073	6.857
770.00	48.305	18.114	35.617	17.088	6.85?

* The units of u are molecules/cm^2, abbreviated here by (#/cm^2).

TABLE 14 $\int_{\nu'}^{\nu} A d\nu$

Sam. No.	HR34	HR35	HR36
Temp (K)	311.	311.	310.
Path (cm)	1648.	1648.	3291.
Conc.	1.00000	1.00000	0.15300
P (atm)	0.048026	0.006079	0.007500
P_e(atm)$_2$	0.062448	0.007903	0.007844
u(#/cm^2)*	1.869E 21	2.366E 20	8.946E 19
ν (cm^{-1})			
705.00	0.	0.	0.
706.00	0.720	0.116	0.084
707.00	1.374	0.228	0.160
708.00	1.991	0.319	0.218
709.00	2.650	0.438	0.293
710.00	3.242	0.536	0.357
711.00	3.865	0.630	0.414
712.00	4.440	0.721	0.470
713.00	4.919	0.791	0.513
714.00	5.514	0.887	0.576
715.00	5.917	0.945	0.615
716.00	6.366	1.008	0.657
717.00	6.882	1.093	0.710
718.00	7.355	1.165	0.758
719.00	8.139	1.322	0.863
720.00	9.097	1.626	1.066
721.00	10.070	2.195	1.487
722.00	10.627	2.281	1.544
723.00	10.932	2.324	1.574
724.00	11.264	2.369	1.607
725.00	11.498	2.401	1.632
726.00	11.869	2.459	1.670
727.00	12.154	2.496	1.699
728.00	12.462	2.538	1.730
729.00	12.887	2.601	1.774
730.00	13.129	2.633	1.799
731.00	13.494	2.687	1.834
732.00	13.890	2.746	1.874
733.00	14.126	2.774	1.895
734.00	14.511	2.831	1.933
735.00	14.861	2.886	1.972
736.00	15.091	2.911	1.987
737.00	15.474	2.967	2.025
738.00	15.863	3.030	2.064
739.00	16.198	3.074	2.091

* The units of u are molecules/cm^2, abbreviated here by (#/cm^2).

TABLE 14 $\int_{\nu'}^{\nu} A d\nu$ (cont.)

Sam. No.	HR34	HR35	HR36
Temp (K)	311.	311.	310.
Path (cm)	1648.	1648.	3291.
Conc.	1.00000	1.00000	0.15300
P (atm)	0.048026	0.006079	0.007500
P_e (atm)	0.062448	0.007903	0.007844
u^e (#/cm^2)*	1.869E 21	2.366E 20	8.946E 19
ν (cm^{-1})			
740.00	16.652	3.148	2.137
741.00	17.168	3.239	2.197
742.00	17.907	3.455	2.341
743.00	18.200	3.498	2.370
744.00	18.433	3.530	2.392
745.00	18.571	3.543	2.401
746.00	18.852	3.581	2.427
747.00	19.076	3.607	2.445
748.00	19.229	3.626	2.455
749.00	19.492	3.660	2.477
750.00	19.710	3.685	2.494
751.00	19.847	3.699	2.503
752.00	20.090	3.733	2.522
753.00	20.282	3.756	2.537
754.00	20.410	3.770	2.545
755.00	20.628	3.799	2.564
756.00	20.807	3.822	2.579
757.00	21.000	3.847	2.593
758.00	21.274	3.889	2.619
759.00	21.405	3.905	2.628
760.00	21.470	3.910	2.633
761.00	21.619	3.931	2.647
762.00	21.747	3.949	2.659
763.00	21.799	3.955	2.662
764.00	21.933	3.974	2.676
765.00	22.036	3.989	2.686
766.00	22.089	3.998	2.692
767.00	22.192	4.015	2.703
768.00	22.279	4.027	2.713
769.00	22.337	4.036	2.720
770.00	22.431	4.050	2.732
771.00	22.504	4.060	2.738
772.00	22.583	4.073	2.747
773.00	22.650	4.084	2.754
774.00	22.696	4.093	2.760
775.00	22.759	4.103	2.769

* The units of u are molecules/cm^2, abbreviated here by (#/cm^2).

TABLE 15 $\int_{\nu'} A\,d\nu$

Sam. No.	HR37	HR38	HR39	HR40	HR41
Temp (K)	311.	311.	310.	311.	311.
Path (cm)	3291.	3291.	3291.	3291.	3291.
Conc.	1.00000	1.00000	1.00000	0.03850	0.00977
P (atm)	7.347368	2.278947	0.769737	10.000000	10.000000
P_e (atm)	9.881420	2.994365	1.004278	10.116406	10.029368
u^e (#/cm^2)*	5.907E 23	1.790E 23	6.023E 22	2.997E 22	7.596E 21
ν (cm^{-1})					
775.00	0.	0.	0.	0.	0.
776.00	1.000	0.987	0.714	0.662	0.249
777.00	2.000	1.966	1.293	1.283	0.477
778.00	3.000	2.951	2.007	1.883	0.699
779.00	4.000	3.929	2.670	2.449	0.899
780.00	5.000	4.902	3.282	2.987	1.086
781.00	6.000	5.880	3.949	3.500	1.262
782.00	7.000	6.828	4.470	3.983	1.427
783.00	8.000	7.770	5.021	4.438	1.582
784.00	9.000	8.706	5.570	4.861	1.726
785.00	10.000	9.592	5.969	5.259	1.859
786.00	11.000	10.482	6.418	5.633	1.986
787.00	12.000	11.345	6.828	5.985	2.100
788.00	13.000	12.149	7.131	6.324	2.213
789.00	14.000	12.968	7.483	6.667	2.331
790.00	15.000	13.768	7.753	7.069	2.470
791.00	16.000	14.708	8.191	7.704	2.768
792.00	17.000	15.702	9.111	8.659	3.546
793.00	18.000	16.702	10.088	9.628	4.211
794.00	19.000	17.692	10.851	10.362	4.504
795.00	20.000	18.567	11.215	10.826	4.659
796.00	21.000	19.422	11.616	11.207	4.786
797.00	22.000	20.257	11.983	11.553	4.913
798.00	23.000	21.061	12.274	11.892	5.032
799.00	24.000	21.947	12.735	12.246	5.155
800.00	25.000	22.775	13.063	12.606	5.260
801.00	26.000	23.613	13.416	12.979	5.410
802.00	27.000	24.516	13.900	13.357	5.548
803.00	28.000	25.334	14.182	13.726	5.675
804.00	29.000	26.214	14.616	14.112	5.809
805.00	30.000	27.099	15.062	14.494	5.941
806.00	31.000	27.908	15.334	14.873	6.065
807.00	32.000	28.788	15.775	15.253	6.195
808.00	33.000	29.628	16.158	15.619	6.315
809.00	34.000	30.415	16.436	15.978	6.440

* The units of u are molecules/cm^2, abbreviated here by (#/cm^2).

TABLE 15 $\int_{\nu'}^{\nu} A d\nu$ (cont.)

Sam. No.	HR37	HR38	HR39	HR40	HR41
Temp (K)	311.	311.	310.	311.	311.
Path (cm)	3291.	3291.	3291.	3291.	3291.
Conc.	1.00000	1.00000	1.00000	0.03850	0.00977
P (atm)	7.347368	2.278947	0.769737	10.000000	10.000000
P_e (atm)	9.881420	2.994365	1.004278	10.116406	10.029368
u^2 (#/cm^2)*	5.907E 23	1.790E 23	6.023E 22	2.997E 22	7.596E 21
ν (cm^{-1})					
810.00	35.000	31.283	16.873	16.332	6.557
811.00	36.000	32.068	17.197	16.661	6.669
812.00	36.998	32.818	17.458	16.980	6.774
813.00	37.995	33.650	17.863	17.295	6.876
814.00	38.991	34.342	18.094	17.576	6.972
815.00	39.986	35.066	18.369	17.851	7.063
816.00	40.981	35.815	18.711	18.110	7.149
817.00	41.974	36.409	18.880	18.338	7.222
818.00	42.965	37.084	19.151	18.565	7.294
819.00	43.953	37.719	19.410	18.768	7.361
820.00	44.933	38.224	19.543	18.950	7.421
821.00	45.908	38.815	19.775	19.126	7.476
822.00	46.873	39.320	19.959	19.281	7.526
823.00	47.820	39.728	20.063	19.423	7.577
824.00	48.760	40.224	20.250	19.555	7.626
825.00	49.673	40.570	20.355	19.675	7.667
826.00	50.574	40.919	20.449	19.782	7.707
827.00	51.477	41.297	20.576	19.883	7.745
828.00	52.410	41.643	20.673	20.017	7.788
829.00	53.402	42.425	21.096	20.277	7.870
830.00	54.345	42.910	21.259	20.424	7.922
831.00	55.195	43.182	21.324	20.516	7.957
832.00	55.992	43.438	21.395	20.590	7.984
833.00	56.748	43.648	21.452	20.655	8.011
834.00	57.471	43.852	21.490	20.717	8.036
835.00	58.182	44.029	21.540	20.779	8.060
836.00	58.871	44.194	21.579	20.836	8.079
837.00	59.546	44.364	21.621	20.893	8.099
838.00	60.210	44.530	21.665	20.944	8.118

* The units of u are molecules/cm^2, abbreviated here by (#/cm^2).

TABLE 16 $\int_{\nu'}^{\nu} A d\nu$

Sam. No.	HR42	HR43	HR44	HR45
Temp (K)	311.	311.	311.	311.
Path (cm)	3291.	3291.	3291.	3291.
Conc.	1.00000	0.15300	1.00000	0.03850
P (atm)	0.192105	0.956579	0.048026	0.988158
P_e(atm)	0.249962	1.000617	0.062448	0.999580
u (#/cm^2)*	1.494E 22	1.138E 22	3.733E 21	2.957E 21
ν (cm^{-1})				
775.00	0.	0.	0.	0.
776.00	0.266	0.299	0.100	0.099
777.00	0.431	0.505	0.156	0.163
778.00	0.685	0.802	0.251	0.257
779.00	0.908	1.035	0.327	0.327
780.00	1.093	1.242	0.394	0.389
781.00	1.313	1.477	0.477	0.463
782.00	1.465	1.636	0.533	0.515
783.00	1.634	1.812	0.593	0.574
784.00	1.815	1.991	0.656	0.632
785.00	1.918	2.100	0.697	0.671
786.00	2.054	2.237	0.752	0.716
787.00	2.180	2.359	0.806	0.756
788.00	2.254	2.433	0.842	0.785
789.00	2.359	2.526	0.883	0.822
790.00	2.432	2.591	0.917	0.855
791.00	2.539	2.715	0.963	0.909
792.00	3.196	3.458	1.425	1.412
793.00	3.911	4.188	1.753	1.750
794.00	4.207	4.481	1.861	1.848
795.00	4.310	4.584	1.897	1.889
796.00	4.441	4.718	1.948	1.938
797.00	4.550	4.843	1.990	1.984
798.00	4.630	4.938	2.018	2.021
799.00	4.777	5.109	2.079	2.084
800.00	4.860	5.223	2.114	2.124
801.00	4.960	5.340	2.149	2.166
802.00	5.108	5.526	2.201	2.229
803.00	5.162	5.610	2.217	2.259
804.00	5.287	5.771	2.260	2.313
805.00	5.419	5.935	2.305	2.370
806.00	5.470	6.005	2.321	2.396
807.00	5.604	6.163	2.365	2.449
808.00	5.714	6.300	2.404	2.492
809.00	5.772	6.381	2.425	2.519

* The units of u are molecules/cm^2, abbreviated here by (#/cm^2).

TABLE 16 $\int_{\nu'}^{\nu} A d\nu$ (cont.)

Sam. No.	HR42	HR43	HR44	HR45
Temp (K)	311.	311.	311.	311.
Path (cm)	3291.	3291.	3291.	3291.
Conc.	1.00000	0.15300	1.00000	0.03850
P (atm)	0.192105	0.956579	0.048026	0.988158
P_e (atm)$_2$	0.249962	1.000617	0.062448	0.999580
u (#/cm^2) *	1.494E 22	1.138E 22	3.733E 21	2.951E 21
ν (cm^{-1})				
810.00	5.898	6.544	2.470	2.571
811.00	5.985	6.660	2.502	2.605
812.00	6.037	6.740	2.520	2.629
813.00	6.157	6.884	2.561	2.673
814.00	6.213	6.953	2.575	2.695
815.00	6.284	7.040	2.598	2.723
816.00	6.388	7.153	2.633	2.759
817.00	6.427	7.202	2.644	2.777
818.00	6.506	7.291	2.674	2.806
819.00	6.582	7.372	2.701	2.835
820.00	6.613	7.409	2.714	2.851
821.00	6.678	7.474	2.737	2.875
822.00	6.728	7.521	2.750	2.888
823.00	6.749	7.542	2.760	2.898
824.00	6.801	7.587	2.785	2.916
825.00	6.830	7.612	2.797	2.928
826.00	6.853	7.634	2.807	2.936
827.00	6.884	7.656	2.810	2.937
828.00	6.905	7.675	2.813	2.941
829.00	7.053	7.803	2.865	2.975
830.00	7.098	7.837	2.876	2.986
831.00	7.113	7.849	2.878	2.992
832.00	7.133	7.861	2.883	2.999
833.00	7.147	7.867	2.886	3.008
834.00	7.159	7.871	2.890	3.015
835.00	7.174	7.876	2.893	3.021
836.00	7.183	7.878	2.895	3.023
837.00	7.196	7.881	2.895	3.023
838.00	7.209	7.881	2.895	3.023

* The units of u are molecules/cm^2, abbreviated here by (#/cm^2).

SECTION 3

H_2O CONTINUUM BETWEEN 330 AND 825 cm^{-1}

This section compares calculated values of the H_2O continuum with experimental values determined previously in our laboratory. It was pointed out in the previous reports that the continuum absorption cannot be determined theoretically from the known line parameters: center position, intensity and half-width. Much of the discrepancy between theory and experiment undoubtedly results from uncertainties in the shapes of the extreme wings of the individual H_2O lines. Self-broadened H_2O lines apparently are shaped differently from N_2-broadened H_2O lines of the same half-width. In addition, the shapes of the extreme wings of the lines show a temperature dependence that is not predictable by simple line-shape theory.

A primary objective of the laboratory work and of the work reported here has been to determine a reliable method of calculating the H_2O absorption by any atmospheric path of interest if the temperature, pressure and H_2O vapor density are known. The AFGL line parameters[1] compilation is to be used as a basis for the calculations. An empirical continuum is being determined to include in the calculations to bring about agreement between theory and experiment. Although much of the discrepancy between theoretical and experimental results is undoubtedly due to errors in the assumed line shapes, we have not attempted to determine a single line shape that would produce the amount of absorption that is observed. Such a task is probably impossible, and it is not likely that a single shape can be used to characterize all lines. Many of the lines that contribute significantly to the absorption at a given wavenumber may be centered more than a hundred cm^{-1} away; thus, the shapes would need to be known far into the wings. Any possible absorption by H_2O:H_2O dimers would also complicate the calculations. Dimer absorption is included, without necessarily being identified as such, in the empirical continuum discussed below.

The experimental data cover a wide range of temperatures, making it possible to study the temperature dependence. Unfortunately, no data have been obtained at reduced temperatures because of the limitations on the maximum H_2O partial pressure that can be achieved at low temperatures. Data covering the wide range of temperatures make it possible to determine the temperature dependence so that some extrapolation to lower temperatures is probably valid.

The following discussion is limited mostly to self-broadening. Analysis of the data on N_2-broadening is continuing; the results will be presented in a future report along with additional data on self-broadening.

LABORATORY MEASUREMENTS

Table 17, repeated here from one of our previous reports,[3] summarizes much

TABLE 17

H_2O CONTINUUM COEFFICIENT FOR
SELF-BROADENING AND N_2-BROADENING

ν cm^{-1}	Multiply all values by 10^{-24} molecules^{-1} cm^2 atm^{-1}				$C_s^o/C_{N_2}^o$	
	C_s^o		$C_{N_2}^o$			
	430 K	296 K	430 K	296 K	430 K	296 K
337.9		16000		1530		10.5
366.0		9790		385*		25.4
389.0		7830		291*		26.9
411.0		6300		140*		45.0
430.0	2400		349		6.9	
433.7	4520	5700	645	160**	7.0	35.6
439.0		5600		160*		35.0
440.1	2950		378		7.8	
448.8	3420	5100	432	117*	7.9	43.6
465.4	2320		296		7.8	
475.1	2640	4300	349	157*	7.6	27.4
482.6	2320	3950	353	166*	6.6	23.6
498.0	1200	3050	110	55.3*	10.9	55.2
531.6	762	2380	62	33.6*	12.3	70.8
559.2	573	1750	44	20.2	13.1	86.6
579.0	972	1680	138	54.7*		30.7
597.0	670	1500	65	26.7*	10.3	56.2
611.4		1170		12.2*		95.9
629.0	330	1100	29	13.0*	13.0	84.6
656.0	219	1000				
683.5	171	930*				
725.5	120	700*				
764.6	97	570*				
790.0	87	540*				
822.0	68	420*				

The estimated errors for C_s^o and C_N^o are $\pm$ 5% except for values marked * and ** which indicate $\pm$ 10% and $\pm$ 20%, respectively.

of the H_2O continuum data on which the following discussion is based. The values listed represent all of the absorption except for that due to lines centered less than approximately 1 cm^{-1} away. The small amount of absorption due to lines centered closer than about 1 cm^{-1} has been accounted for and subtracted from the observed absorption. Thus, the lines contributing to the absorption represented are centered several half-widths from the point of observation so that the contribution to the absorption coefficient by each line is proportional to the pressure. (See Equation (7)).

At 296 K, C_S^o is generally much greater than at the higher temperature, a result that agrees with previous results[8,9] in other spectral regions. If the major portion of the absorption at the wavenumbers investigated for pure H_2O is due to the extreme wings of the absorption lines, these results indicate that the influence of temperature on the shapes of the self-broadened lines is greater than that predicted by simple theories on collision broadening. This unpredictably strong negative temperature dependence provides a basis for attributing the absorption to dimers because it is known that the concentration of dimers of any molecule decreases rapidly with increasing temperature. However, some of the results shown below in this report, as well as other results of ours shown previously, indicate that the extreme wings of absorption lines have an unpredictably strong negative temperature dependence. Therefore, it seems likely that some of the absorption attributed by many to dimers may be due to the extreme wings of lines with shapes that are not well understood.

COMPARISON OF MEASUREMENTS WITH THEORY

Figure 14 compares a segment of a typical experimental spectrum with a corresponding spectrum calculated for the same sample of pure H_2O. The calculated spectrum represented by the upper curve was computed by a line-by-line method with the AFGL line parameters serving as the basis. The spectrum was then "degraded" to correspond to the finite spectral slitwidth (0.4 cm^{-1}) of the spectrometer used to scan the laboratory spectrum. Laboratory measurements agree quite well in the narrow regions of strong absorption with this calculated spectrum based on the line-by-line method. Serious discrepancies occur, however, in the narrow regions of weak absorption between the absorption lines.

In order to produce better agreement between calculated and observed spectra, we have added an empirical continuum to the calculated absorption; the result is represented by the dotted curve in Figure 14. The empirical continuum contains no spectral structure and is nearly constant over the spectral interval shown.

---

8. Darrell E. Burch, "Investigation of the Absorption of Infrared Radiation by Atmospheric Gases." Semi-Annual Technical Report, Contract F19628-69-C-0263. Aeronutronic Report No. U-4784, Jan. 1970.

9. Darrell E. Burch, David A. Gryvnak and Gerald H. Piper; "Infrared Absorption by H_2O and N_2O." Final Report Contract No. F19628-73-C-0011. Aeronutronic Report No. U-6026, July 1973.

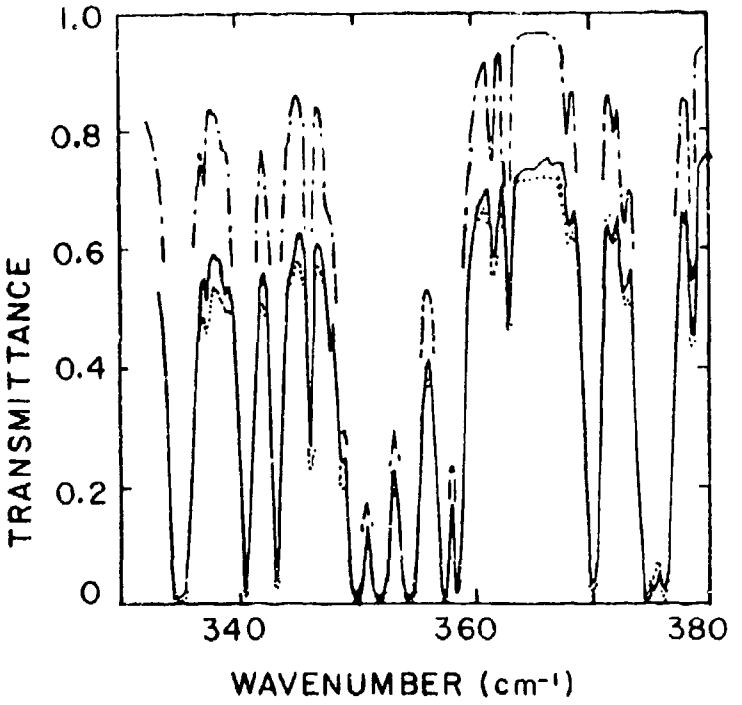

Figure 14. Comparison of calculated spectra with a laboratory spectrum of pure H_2O. The solid curve represents the laboratory measurement; the upper curve represents the calculated spectrum based on the Lorentz line shape. An empirical continuum has been added to the calculated spectrum to produce the dotted curve. P = p = 0.0207 atm; T = 296 K, and u = 1.48 $\times 10^{21}$ molecules/cm^2.

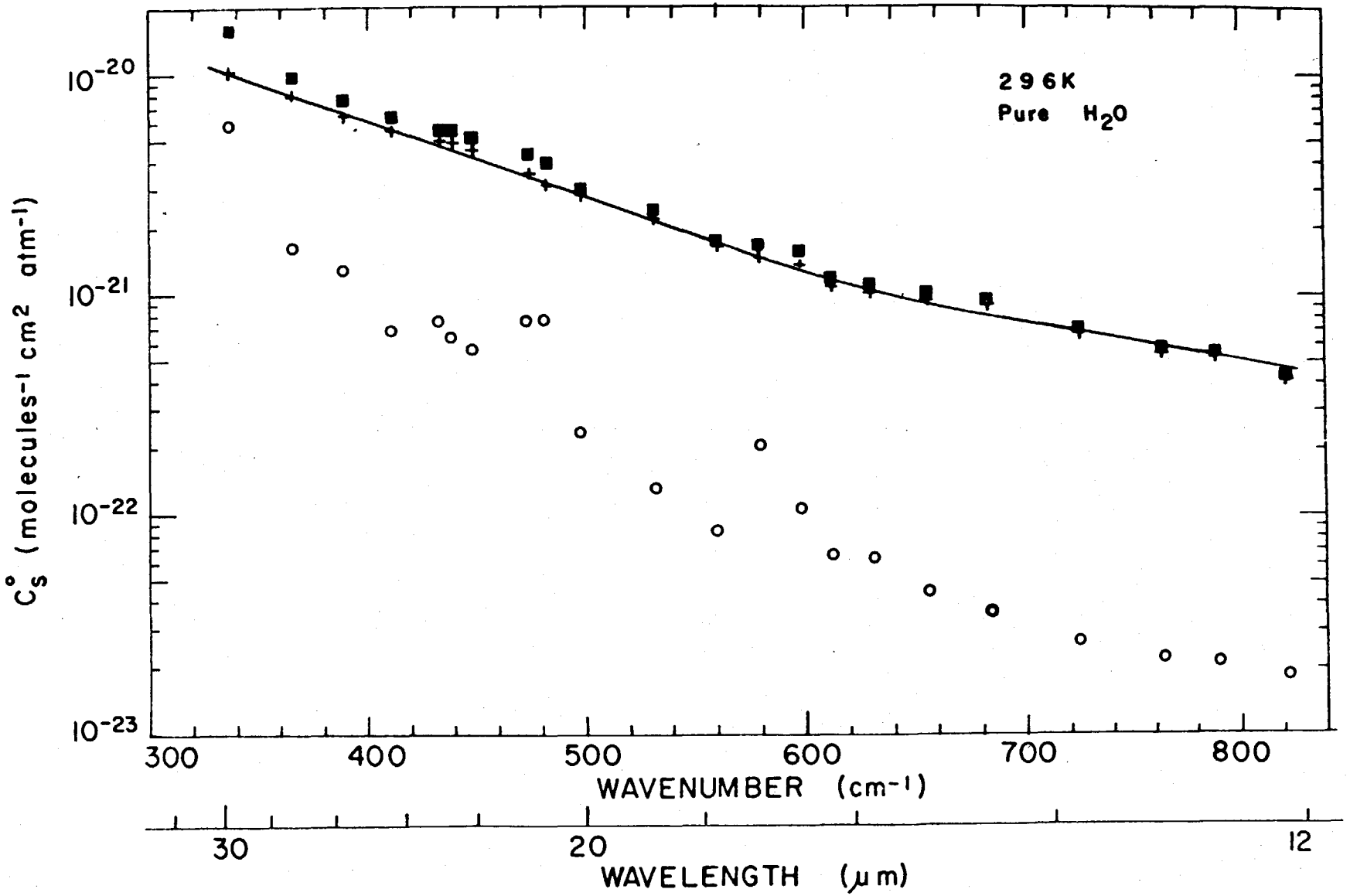

Figure 15. Spectral plot of C_s^o for H_2O samples at 296°K. ■ , laboratory measurements; O, values calculated by summing the contributions by all H_2O lines centered more than 1 cm^{-1} from the wavenumber of measurement. The +'s and the curve represent $^{e}C_s^o$, the empirical continuum.

Addition of the empirical continuum has only a very small influence on the calculated spectrum near the centers of the absorption lines; the most influence is observed in the narrow windows between the lines. Although addition of the empirical continuum greatly improved the agreement with the laboratory measurements, it is apparent that slightly better agreement would be obtained in this spectral interval if somewhat less empirical continuum had been included. Much of the remainder of this section deals with the determination of an empirical continuum for pure H_2O in the 300-800 cm^{-1} region.

The solid squares in Figure 15 represent values of C_s^o obtained from laboratory measurements as described above at wavenumbers where most of the absorption is due to lines centered more than approximately 2 cm^{-1} from the point of measurement. Values calculated without any empirical continuum are represented by the circles; these values were found by including the calculated contributions for all H_2O lines. Computer time was greatly reduced by treating all of the lines centered above 1000 cm^{-1} as a single, equivalent line centered at 1595 cm^{-1}. A previous calculation indicated only a very small contribution in the 300-800 cm^{-1} region by these lines for which $\nu_o > 1000$ cm^{-1}. Therefore, representing this small contribution by a single line introduced negligible error in the calculations. A Lorentz line shape was assumed for all lines. As discussed previously, contributions by lines centered closer than 1 cm^{-1} from a point of calculation are not included in either the laboratory data or the calculated values of C_s^o. Each of the values represented by the +'s was obtained by subtracting the calculated value represented by the circle from the corresponding laboratory value represented by a solid square. Thus, a + sign represents the value of "extra" continuum, or empirical continuum, required to bring about agreement between calculated and experimental values.

The curve drawn through the +'s represents the empirical continuum for pure H_2O samples at 296 K. Values from this smooth curve are used to represent the empirical continuum coefficient, ${}^eC_s^o$, in transmission calculations. At any wavenumber, the total attenuation coefficient for pure H_2O (no N_2 or other broadening gas) is given by

$$\kappa(\text{molecules}^{-1}\text{cm}^2) = \Sigma k(\text{for all lines}) + {}^eC_s^o\, p. \qquad (12)$$

In this last step of the calculation, all of the lines, including those centered within 1 cm^{-1}, are included. The contribution by the empirical continuum is equal to the pressure of H_2O vapor times the normalized empirical continuum coefficient.

Figures 16 and 17 show data similar to those in Figure 15, except each figure corresponds to a different sample temperature. Data at the elevated temperatures, 338 K and 430 K, were not obtained over the entire spectral region included in the study at 296 K. The empirical continuum curves in Figures 15-17 have been redrawn together in Figure 18 for easy comparison. A very strong negative temperature dependence is apparent. For example, near 500 cm^{-1} the empirical continuum represented by Figure 18 is only approximately 20% as great at 430 K as it is at 296 K. The calculated line contribution (represented by the circles)

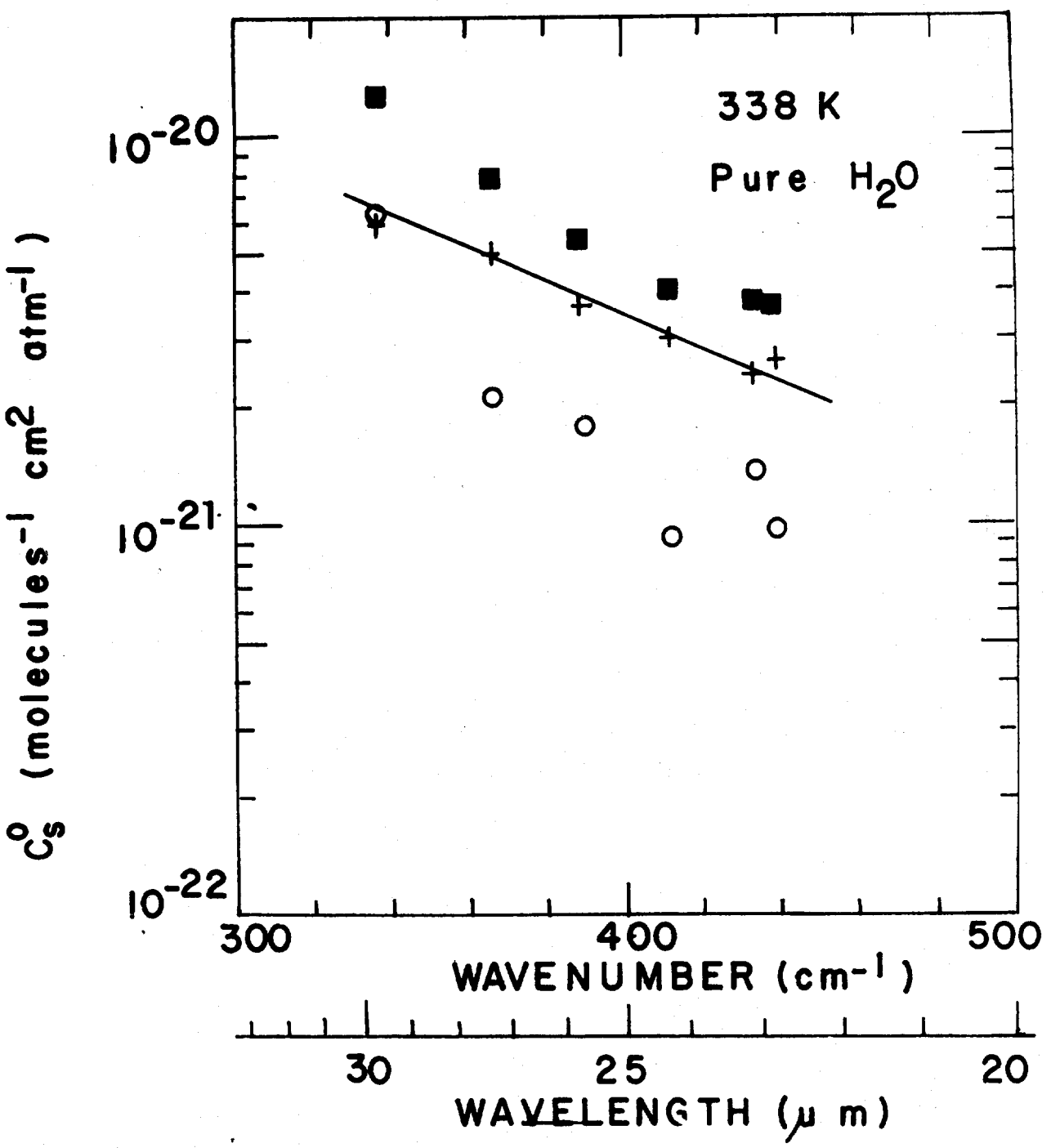

Figure 16. Spectral plot of C_s^o for H_2O samples at 338°K. ■ , laboratory measurements; ○ , values calculated by summing the contributions by all H_2O lines centered more than 1 cm^{-1} from the wavenumber of measurement. The +'s and the curve represent $^{e}C_s^o$, the empirical continuum.

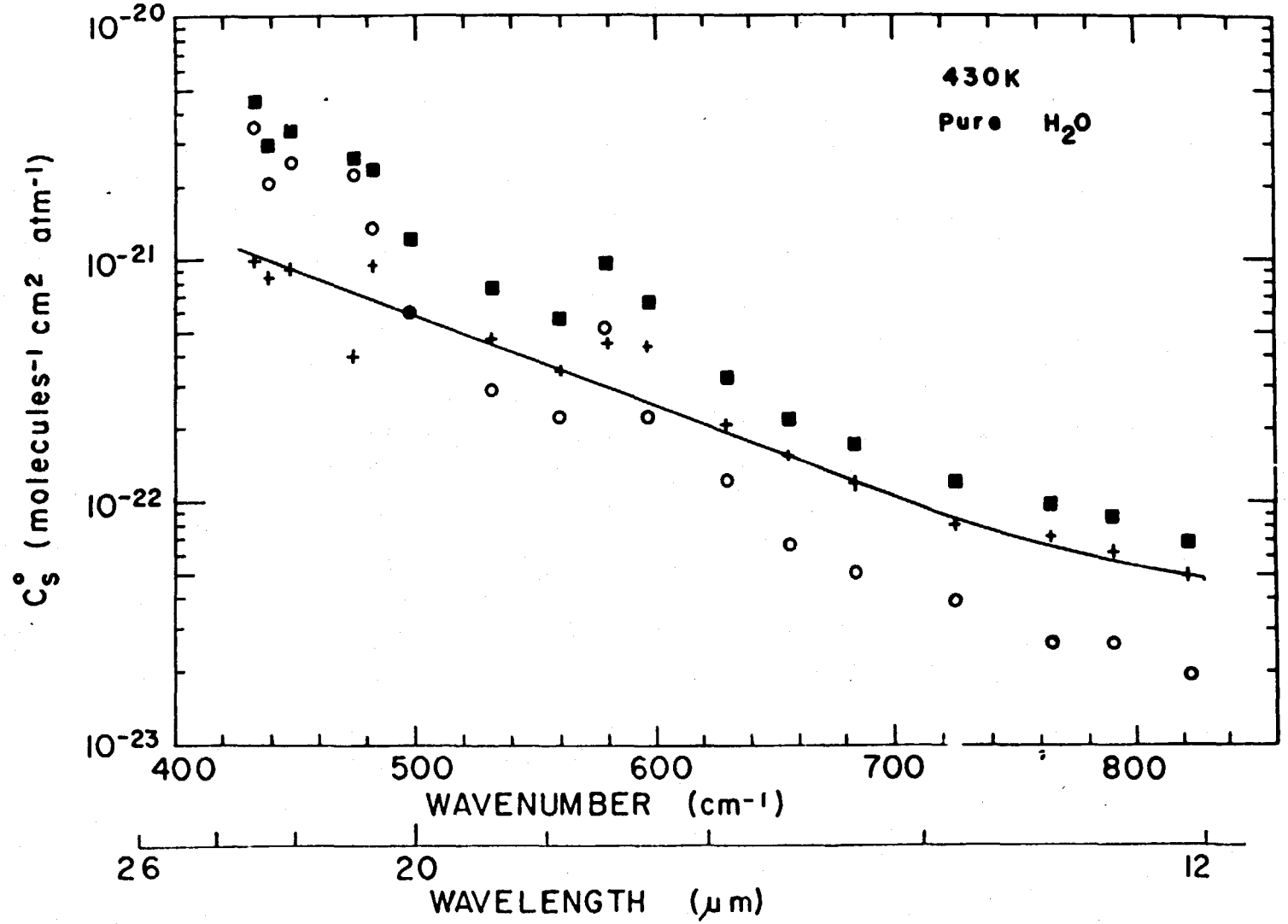

Figure 17. Spectral plot of C_s^o for H_2O samples at 430°K. ■, laboratory measurements; ○, values calculated by summing the contributions by all H_2O lines centered more than 1 cm^{-1} from the wavenumber of measurement. The +'s and the curve represent $^eC_s^o$, the empirical continuum.

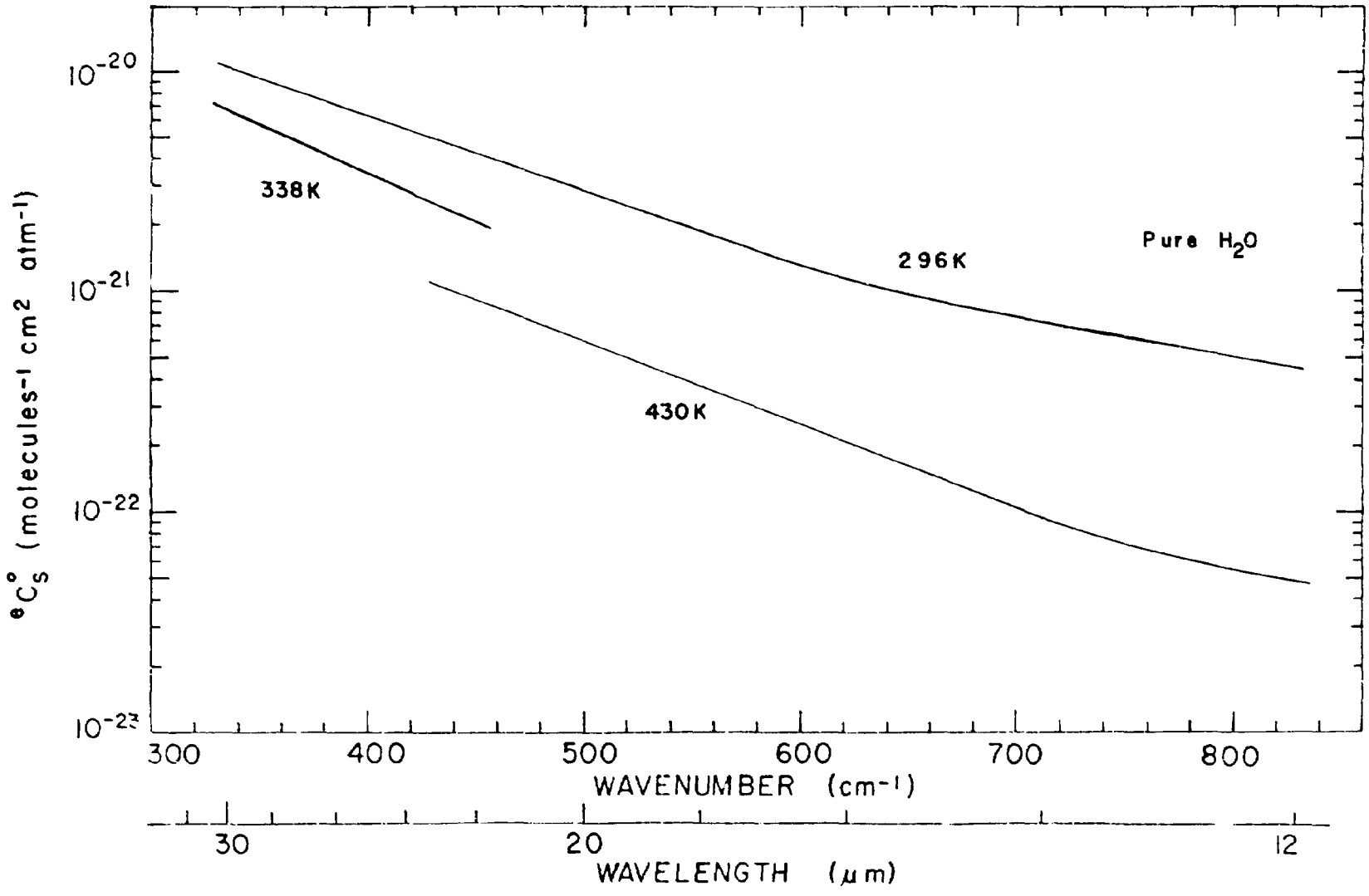

Figure 18. Spectral plots of the empirical continuum for pure H_2O samples at three different temperatures.

increases with increasing temperature because the intensities of most of the lines in the 300-800 cm^{-1} region increase with increasing temperature. Thus, as the temperature increases, the empirical continuum is responsible for a decreasing fraction of the absorption.

It is of interest that nearly all of the +'s in either Figure 15 or 16 fall within +10% of the corresponding smooth curve based on the points. The deviation from the smooth curve is greater for the 430 K samples represented by Figure 17 because the laboratory data are somewhat less accurate and the empirical continuum produces a smaller fraction of the absorption. Note that many of the calculated values represented by the circles would not fall near a single smooth curve. The points that would fall furthest above a smooth curve represent wavenumbers where strong absorption lines are centered within about 3-10 cm^{-1}; therefore, the absorption is greater than at other wavenumbers that are further from very strong lines. These points of greater absorption were included to help in providing information about the nature of the "extra" absorption represented by the empirical continuum and about the relative shapes of self-broadened and N_2-broadened H_2O lines. It is informative that essentially the same amount of empirical continuum is required to provide agreement between theory and experiment at the wavenumbers of very low absorption as at those points where the calculated absorption coefficient may be 2-5 times greater.

Although the source of the extra absorption, represented here by the empirical continuum, cannot be determined unambiguously, a few of its characteristics can be inferred. The strong negative temperature dependence of the continuum coefficient observed in the spectral region studied here, as well as in the 8-12 μm window, has led many people to believe that the absorption is due to dimers, or to clusters of several H_2O molecules. However, it is significant that no spectral structure has been observed in the infrared that can be assigned with certainty to dimers. Absorption by the extreme wings of individual H_2O lines probably should not be ruled out as a major source of the continuum on the basis that present line shape theories do not predict the strong negative temperature coefficient that is observed. In other laboratory studies of the absorption by H_2O, CO_2, and N_2O, we have found that absorption by the extreme wings of the lines decreases faster with increasing temperature than is predicted by present theories. The temperature dependence observed for CO_2 and N_2O continuum absorption is less than has been observed for H_2O, nevertheless it is quite significant.

If the empirical continuum is, in fact, due to "super-Lorentzian" absorption by the lines, the super-Lorentzian behavior must occur over a large portion of the extreme wings of each line. For example, assume that each line was super-Lorentzian only over the region 5 $cm^{-1} < |\nu-\nu_0| < 10$ cm^{-1} and Lorentzian, or sub-Lorentzian, elsewhere. In this case, the empirical continuum would not be represented by a smooth curve; instead, it would vary with wavenumber, depending on the intensities of the lines centered within the 5-10 cm^{-1} range. The empirical continuum represented by the curve in Figure 15 decreases gradually with increasing ν in much the same way as the average intensities of the lines decrease. This strongly suggests that the source of the continuum is related directly to the lines.

SECTION 4

REFERENCES

1. R. A. McClatchey, W. S. Benedict, S. A. Clough, D. E. Burch, R. F. Calfee, K. Fox, L. S. Rothman, and J. S. Garing; "AFCRL Atmospheric Absorption Line Parameters Compilation", AFCRL-TR-73-0096, 26 January 1973. (Associated with this report is a magnetic tape listing the line parameters.)

2. David A. Gryvnak, Darrell E. Burch, Robert L. Alt, and Dorianne K. Zgonc; "Infrared Absorption by CH_4, H_2O and CO_2", Final Report No. AFGL-TR-76-0246 on Contract F19628-76-C-0067. Aeronutronic Report No. U-6275, December 1977.

3. Darrell E. Burch, David A. Gryvnak, and Francis J. Gates; "Continuum Absorption by H_2O Between 330 and 825 cm^{-1}", Final Report No. AFCRL-TR-74-0377 on Contract F19628-74-C-0069. Aeronutronic Report No. U-6095, September 1974.

4. Darrell E. Burch, David A. Gryvnak, and John D. Pembrook; "Infrared Absorption by H_2O, NO_2, and N_2O_4", Final Report No. AFCRL-TR-75-0420 on Contract No. F19628-75-C-0049. Aeronutronic Report No. U-6159, September 1975.

5. E. P. Gross, Phys. Rev. 97, 395 (1955).

6. W. S. Benedict, Inst. for Molecular Physics, College Park Maryland, 90742; R. Calfee, Wave Propogation Labs., Environmental Research Labs, National Oceanic Atmospheric Administration, Boulder Colorado 80302 (Private Communication).

7. S. R. Drayson, "A Listing of Wavenumbers and Intensities of Carbon Dioxide Absorption Lines Between 12 and 20 μm". Technical Report 036350-4-T, National Aeronautics and Space Administration, Contract No. NSR 23-005-376, May 1973.

8. Darrell E. Burch, "Investigation of the Absorption of Infrared Radiation by Atmospheric Gases." Semi-Annual Technical Report, Contract F19628-69-C-0263. Aeronutronic Report No. U-4784, Jan. 1970.

9. Darrell E. Burch, David A. Gryvnak and Gerald H. Piper; "Infrared Absorption by H_2O and N_2O." Final Report Contract No. F19628-73-C-0011. Aeronutronic Report No. U-6026, July 1973.